Summer 2019

Springtime benthic fluxes in the Salish Sea: Environmental parameters driving spatial variation in the exchange of dissolved oxygen, inorganic carbon, nutrients, and alkalinity between the sediments and overlying water

Emma I. Rigby
Western Washington University, emma.i.rigby@gmail.com

Recommended Citation
Rigby, Emma I., "Springtime benthic fluxes in the Salish Sea: Environmental parameters driving spatial variation in the exchange of dissolved oxygen, inorganic carbon, nutrients, and alkalinity between the sediments and overlying water" (2019). *WWU Graduate School Collection*. 903.
https://cedar.wwu.edu/wwuet/903

Springtime benthic fluxes in the Salish Sea: Environmental parameters driving spatial variation in the exchange of dissolved oxygen, inorganic carbon, nutrients, and alkalinity between the sediments and overlying water

By

Emma Rigby

Accepted in Partial Completion
of the Requirements for the Degree
Master of Science

ADVISORY COMMITTEE

Dr. David Shull, Chair

Dr. Brooke Love

Dr. Robin Matthews

GRADUATE SCHOOL

David Patrick, Interim Dean of Graduate School

Master's Thesis

Emma Rigby

July 2019

Springtime benthic fluxes in the Salish Sea: Environmental parameters driving spatial variation in the exchange of dissolved oxygen, inorganic carbon, nutrients, and alkalinity between the sediments and overlying water

A Thesis
Presented to
The Faculty of
Western Washington University

In Partial Fulfillment
Of the Requirements for the Degree
Master of Science

By
Emma Rigby
July 2019

Abstract:

Recent decades have seen changes to biogeochemical cycles in the Salish Sea, including alterations in water column nutrients, an expansion of hypoxic zones, and bottom water acidification. Marine sediments can be a major contributor to these biogeochemical cycles by exchanging solutes with bottom water. In an effort to understand the sediment biogeochemistry of the Salish Sea further, benthic fluxes of dissolved oxygen (DO), dissolved inorganic carbon (DIC), pH, total alkalinity (TA), and nutrients (ammonium, nitrate+nitrite, phosphate, silicate) between the sediment and the overlying water were directly measured using incubated flux cores at 42 sites in April and early May 2018. Explanatory variables describing bottom water conditions (salinity, temperature, DO, DIC, pH, and TA), sediment properties (grain size, total organic carbon, and C:N ratio), and site depth at the time of sampling were also collected. Denitrification estimates for each station were made using the benthic fluxes and estimates of C:N ratios of organic matter suspended in bottom water near each station.

Benthic fluxes varied considerably across the Salish Sea and high variability was observed between core replicates. In general, DO fluxes were larger than DIC fluxes and we attributed this to the oxidation of reduced compounds stored in sediments. The ratio phosphorus to DIC fluxes were less than the Redfield ratio, indicating phosphorus storage in the sediments. At all but two sites denitrification was present, with a median rate of 1 mmol m^{-2} d^{-1}. Using canonical redundancy analysis, the spatial variation observed in benthic fluxes and denitrification rates was determined to be primarily driven by water column depth and bottom water DO.

Spatial variation was also observed in the estimations of sediment contribution to water column biogeochemistry in Puget Sound basins. Denitrification rates were estimated to remove 11% of the dissolved inorganic nitrogen (DIN) supplied to the bottom water in Hood Canal, while in the Central Basin only 1% was removed. This difference was due to the long bottom water residence time in Hood Canal, where the denitrification can have a larger impact on bottom water DIN concentrations as the water slowly moves through the basin. Nearly all of the particulate phosphorus that reached the seafloor during the early spring was estimated to be stored in the sediment. Sediment oxygen uptake was found to account for approximately 80% of the bottom water DO removal in the South Basin compared to 21 – 35% in the other basins. The sediments play a large role in the South Basin because it is shallow.

This spatial study illuminates the varying contributions that sediments make to the functioning of Salish Sea biogeochemistry. Seasonal benthic flux measurements should be made to further understand and quantify the influence that sediments have on water column biogeochemistry in the Salish Sea.

Acknowledgements:

My first and foremost thanks goes to my adviser, Dr. David Shull. Thank you for the never-ending support of my studies and research, your positive and motivating energy, your patience, and immense knowledge. I'm especially grateful for *all* the time you generously spent to make me a better scientist. Warmest thank you's to my committee members Dr. Brooke Love and Dr. Robin Matthews for your ideas and insight, constructive feedback, and answering my questions with such eagerness.

This research would not have been possible without assistance of the Marine Sediment Monitoring Team at Washington State Department of Ecology. I am sincerely grateful for the time and work you all put in to help me to collect my cores and process my samples on deck, as well as all of the behind the scenes work it took to get me on the cruise. Your enthusiasm and eagerness to learn is incredibly inspiring to me as a young women scientist. Maggie Dutch, Valerie Partridge, Sandy Weakland, Danny Burgess, Angela Eagleston, Carol Maloy, and Juhi LaFuente – thank you! I am also very grateful for the Gravity Marine Consulting crew, especially Shawn Hinz and Ryan McEliece, who were incredibly innovative and helped me problem solve on everything from the Niskin to fixing a car battery. Thank you for teaching me on board, the friendly encouragement, and cleaning up all my mud at the end of the day.

The faculty and staff at Shannon Point Marine Center made my time at WWU a complete success. Thank you to Gene McKeen for helping me sort out any logistical and equipment issues, to Nate Schwartz and Jay Dimond for operating the research vessels and helping with sample collection for the seasonal portion of this study, and to Horng-Yuh Lee for the support in the chemistry lab and for answering all my questions. A huge thank you to the Huxley staff on campus as well. Ed Weber, Rose Kawczynski, Alona Christman, and Bonnie Drews, you rock! Thank you also to Charlie Wandler in Science and Technical Services for helping me to work through my samples on the Flame AA.

Thank you to the two undergraduate interns that put their time and hard work into this project, Audrey Mechtenberg and Ryan McGinnis.

A special thank you to my friends, especially the amazing Bellingham community I seemingly walked into. Your encouragement and perspective is sincerely appreciated. A heart-felt thank you to my fellow graduate students Caroline Walls, Rob Beck, and Amy Irons for your compassion and friendliness.

Finally, thank you to my family for the relentless support throughout my life and whole academic journey. Mom, thank you so much for the motivating visits and guidance. A very big thank you to my best friend and most enthusiastic supporter, Javier Santana. Thank you for all of the laughs and late night coffee, listening to me about anything and everything, and your endless encouragement for me to reach for my goals.

Funding for this project was provided by Washington State Department of Ecology, the Jerry Flora summer research grant, Huxley College of the Environment, and WWU Graduate School.

Table of Contents:

List of Tables

List of Figures

Introduction:

In shallow coastal systems, sediments play an essential but often overlooked role in the biogeochemical cycling of organic carbon and nutrients (Arndt et al. 2013, Nixon 1981). The shallow depths on continental shelves, usually less that 200m, allow for large amounts of reactive organic matter produced in surface water to be exported to seafloor (Middelburg et al. 1996, Suess 1980). Organic matter deposition on the seafloor enhances faunal and microbial respiration rates in the sediments and leads to increased exchanges of solutes and dissolved gases between the sediments and the overlying water (Burdige 2006, Suess 1980). A benthic or sedimentary flux is defined as the movement of solutes between the sediment and bottom water per unit area per unit time. Enhanced benthic fluxes in coastal systems make sediments important for biogeochemical cycling.

The movement of nitrogen through a marine system is a prime example of a biogeochemical cycle that is heavily influenced by sediments, as well as one that has changed over recent years. Nutrient loading in the form of excess dissolved inorganic nitrogen (DIN) can be a common problem in coastal systems leading to eutrophication and shifts in planktonic communities (Smith et al. 2006, Rabalais et al. 2009). Sedimentary denitrification is the primary removal mechanism of DIN from marine systems (Burdige 2006). Two mechanisms of denitrification are observed in marine sediments. These are nitrate reduction, a form of anaerobic respiration that converts bioavailable nitrate (NO_3^-) into nitrogen gas (N_2), and anammox, a respiratory pathway that converts ammonium (NH_4^+) and nitrite (NO_2^-) to N_2 (Babbin et al. 2014, Devol 2015). I use the term denitrification to describe the conversion of DIN to N_2 by either of these mechanisms. Because N_2 is a mostly unusable nitrogen species in estuarine and coastal waters (Marino and Howarth 2016), sedimentary denitrification effectively removes DIN from these systems. Although N_2 can be fixed back into DIN in the water column by cyanobacteria, such as diazotrophs, their relative influence is small in areas with large inputs of DIN (Sohm et al. 2011, Sutton et al. 2013). Denitrification in marine sediments can remove 12 - 81% of the total reactive nitrogen input from organic matter, with the highest rates found in areas of high nutrient and low oxygen concentrations (Burdige 2006). Quantifying the rates of sedimentary denitrification, as well as the fluxes nitrogen species like ammonium and nitrate, are necessary in order to understand the coastal marine nitrogen cycle.

Eutrophication can lead to the development of large, and sometimes persistent, phytoplankton blooms (Smith et al. 2006, Rabalais et al. 2009). Greater than normal concentrations of organic matter from these blooms supports an increase in bottom water respiration, which can cause a reduction in water column dissolved oxygen (DO) concentration. Hypoxia, DO concentrations less than 2 mg L^{-1}, has become more frequent in many coastal systems (Rabalais et al. 2010). Hypoxia can be devasting to biological communities and in the worst case scenarios, “dead zones” occur where few multicellular organisms exist due to the lack of oxygen available (Newton et al. 2007). Furthermore, hypoxic conditions in the water column can be exacerbated by oxygen consumption by marine sediments. Faunal and microbial respiration in sediments, as well as the oxidation of reduced compounds within the sediment, remove DO from bottom water (Burdige 2006, Norkko et al. 2015). As hypoxia becomes more common, it is imperative to quantify how much DO is removed by marine sediments to model the response of coastal ecosystems to eutrophication accurately.

When reduced bottom water DO concentrations are present, sediment biogeochemistry is also impacted (Middelburg and Levin 2009). When DO concentration is low, DO fluxes into the sediment decrease due to the reduced oxygen gradients across the sediment-water interface

(Middelburg and Levin 2009). The ammonium flux out of the sediment significantly increases in bottom water with low DO concentrations due to conditions that prevent nitrification (the microbial conversion of ammonium to nitrate; Middelburg and Levin 2009). Phosphate fluxes out of the sediment are also enhanced due the dissolution of iron oxides that bind phosphorus (Sundby et al. 1992). Additionally, low bottom water DO concentrations leads to an overall reduction in the amount of aerobic respiration occurring in the sediments, while anaerobic respiration increases (Middelburg et al. 1996).

Elevated DIN concentrations in the water column can also cause phytoplankton communities to shift from diatom-dominated taxa toward flagellate-dominated taxa (Turner et al. 1998). Phytoplankton communities dominated by flagellates export less organic carbon to the sediments due to more efficient carbon metabolism in the water column (Turner et al. 1998). This, in turn, can both reduce and alter the composition of the food supply to the seafloor and affect the health of the benthic communities below (Grebmeier et al. 1988). The release of dissolved inorganic carbon (DIC) from sediments approximates of the rate of organic carbon supply to the sediment (minus organic carbon preservation and burial) and the rate of sedimentary organic matter respiration (Burdige 2006). While organic carbon mineralization primarily produces DIC flux, this flux is also influenced by the production or dissolution of calcium carbonate (Burdige 2006). The measurement of benthic DIC fluxes provide additional information on the changing dynamics of organic matter exported from the surface and the varying respiration rates of organic matter in the sediment.

The general increase in the acidity of ocean water is amplified in many coastal areas due to the upwelling of corrosive waters (Feeley et al. 2010) and high rates of ecosystem respiration (Lowe et al. 2019, Wallace et al. 2014). The response a marine system will have to ocean acidification has yet to be fully understood particularly due to the various components that influence the carbonate system. Sediments can either contribute to the total alkalinity (TA) of the bottom water and increase the buffering capacity, or can do the opposite and reduce it. (Brenner et al. 2016, Krumins et al. 2013). The release of TA from the sediments is mainly produced through DIC released via respiration, the uptake of hydrogen ions, and the release of anions and weak bases created in some types of anaerobic respiration (Burdige 2006). Geochemical reactions and the dissolution or creation of calcium carbonate can also contribute to the TA fluxes into or out of the sediment (Burdige 2006). The carbonate system is also influenced by the sedimentary production of hydrogen ions. Various biological activities and chemical reactions in the sediments produce hydrogen ions that add to the acidity of the bottom water. The buffering capacity and acidity of the bottom water may be enhanced or depleted by sediments, which is an additional reason to determine function of sediments in an estuary.

Similar to many other estuaries, the Salish Sea is undergoing nutrient concentration alterations, increases in the occurrences of hypoxia, as well as ocean acidification. Located in the Pacific Northwest of the United States and Canada, the Salish Sea transcends political borders and encompasses the water bodies of Puget Sound, the Strait of Juan de Fuca, and the Strait of Georgia. Salish Sea DIN concentrations have been highly variable over recent years (PSEMP Marine Waters Workgroup 2018). Nitrogen budgets for the region suggests that eutrophication is not a pressing issue in the region due to the large supply of nutrient rich bottom water located beneath the pycnocline (Mackas and Harrison 1997, Sutton et al. 2013). This bottom water that flows into the Salish Sea from the Pacific Ocean, is estimated to contribute 85% of the DIN supply, while rivers account for approximately 5%, and all other sources, including the atmosphere and wastewater treatment plants, are less than 1% each (Sutton et al. 2013). Despite this small contribution from anthropogenic inputs (e.g. waste water treatment plants), Puget Sound receives more than double its natural load of land sourced DIN, some of which is released during time periods when nutrients limit phytoplankton growth (Mohamedali et al. 2011). Hypoxia is also an increasingly important problem. Over the past 20 years, there has been a rise in the number, size, and duration of low oxygen events in the Hood Canal basin and other bays and inlets in the Salish Sea (Batker et al. 2008). An additional threat to the marine life in the Salish Sea is ocean acidification. Anthropogenically produced carbon is estimated to account for 24 - 49% of the drop in pH in the bottom water of Hood Canal basin compared to pre-industrial pH values (Feeley et al. 2010). The supply of acidic bottom water from the North Pacific Ocean makes the Salish Sea even more vulnerable to the effects of anthropogenic acidification (Feeley et al. 2010).

Despite the ongoing biogeochemical changes in the Salish Sea, there is limited knowledge on the contribution that sediments make to the chemistry of the water column. The relationship between sediment and the water column DO was last quantified on a broad scale in Puget Sound more than 50 years ago (Pamatmat 1971). Pamatmat’s study quantified benthic oxygen uptake seasonally at 22 stations in Puget Sound, primarily focused in the Central and South Basins. He made no measurements of DIC or nutrients fluxes to or from the sediment. Rates of denitrification have been estimated in just a few locations in Penn Cove located in Whidbey Basin and in southern Hood Canal (Brandes and Devol 1997, Engström et al. 2009). In 2015, nutrient fluxes were measured at a limited number of stations in the southern region of the Strait of Georgia (Belley et al. 2016). The lack of a broad scale survey of sediment geochemistry in the Salish Sea is a significant gap in the understanding of ecosystem function, which is particularly problematic given the rapid geochemical changes that have been observed over recent years (e.g. Feeley et al. 2010).

To fill this gap, I conducted a survey of the spatial variation of springtime benthic fluxes throughout Puget Sound and adjacent Salish Sea regions in Washington State. The sampling stations extended from Olympia to the Canadian border and included inlets, bays and major basins (Figure 1). These stations are the same locations that are monitored by the Washington State Department of Ecology's (DOE) Marine Sediment Monitoring Team (MSMT) for annual long-term sampling of benthic community structure and bulk sediment properties. This network of stations includes 10 original stations chosen at the program's inception in 1988, 12 stations that coincide with monitoring by DOE's Marine Waters Monitoring Program or the Washington Department of Fish and Wildlife's Toxics-focused Biological Observing System, and 28 stations that were randomly chosen based on a generalized random tessellation stratified (GRTS) multi-density survey design (Stevens and Olsen 2004). The station numbers I used for this study were those used by the MSMT.

Measuring benthic fluxes spatially and temporally can inform where the organic matter supply is the highest and how the supply changes seasonally and annually. Springtime, prior to the spring bloom, was the ideal time period to measure these benthic fluxes because they are representative of a majority of the year, approximately five to six months, when organic carbon supply is low. From late October (post-fall bloom) to late April (pre-spring bloom), organic carbon supply to the sediments is limited due to low surface water productivity. It has been well documented that benthic fluxes exhibit seasonal variability, generally in-sync with primary productivity (e.g. Belley et al. 2016, Horak et al. 2013). In coastal waters, the benthic fluxes of DO and DIC measured during the late fall to early spring generally increase by a factor of two to three, depending on the year (Dollar et al. 1991, Hammond et al. 1985, Giblin et al. 1997). Instead of capturing these natural cycles and variations, these springtime benthic flux measurements establish a contemporary baseline, identify spatial patterns of benthic fluxes within the region, determine which environmental parameters drive the variation in benthic fluxes, and enable a better understanding the role sediments play in the biogeochemical cycling in the Salish Sea.

Methods:

Core and Bottom Water Collection

To quantify springtime benthic fluxes in the Salish Sea, the MSMT and I attempted to sample a total of 50 stations in April and early May 2018. Of the 50 targeted stations, we collected sediment cores and bottom water samples from 42 stations.

A Haps corer was deployed at each of the stations to collect two undisturbed, 30-cm long cores filled about two-thirds of the way with sediment and one-third with overlying water. The height of the overlying water ranged from 6-cm to 20-cm. The replicate cores were taken on average 7.5m from one another. If a sediment core had a disturbed sediment surface and murky overlying water due to sediment disruption, the core was not used in the study and another core was taken to replace it. If no usable cores were obtained after a series of attempts, the site was removed from the study.

After collection, the cores were carefully extruded and transferred into 8.2-cm diameter polyethylene terephthalate flux cores. These were capped with PVC lids equipped with polybutadiene O-rings, sampling ports to extract the overlying water, and a magnetic stir bar to homogenize the overlying water. I ensured that no air bubbles were visible in the overlying water once capped to prevent an alteration in the gas content of the water. The flux cores were then incubated at near bottom-water temperature (~10ºC) in modified coolers filled with sea water for 18 to 24 hours (Figure 2). The temperature in the incubators was kept stable within a 2°C range of 10ºC by using a thermostatted cold finger (a refrigerator coil with an attached flexible probe filled with coolant). The chilled seawater circulated through the incubators and around the cores by means of propellers rotated by a small motor on the lid, which also turned horseshoe magnets that rotated the magnetic stir bars at a rate of one revolution per second (Figure 2). The incubators also prevented any light penetration so that photosynthesis could not take place in the flux cores. Nearly all of the flux cores in my study were incubated on board the research vessel. Due to logistics, three stations (40013, 40025, and 305R) were incubated at *in situ* temperature (10ºC) in a cold room after core collection was completed.

At each of the stations, bottom water samples (one to four meters above the sediment) were collected using a Niskin bottle attached either to the Haps corer frame or to a cable. Bottom water DO was immediately measured on deck using PreSens optode spots affixed on the inside of two 25mL glass scintillation vials. The optode spots in the vials were calibrated prior to the cruise using a two point calibration of saturated and 0% oxygen solutions. The saturated solution was made by leaving nanopure water uncapped for 12+ hours to obtain DO saturation, whereas the 0% oxygen solution was made by adding sodium sulfite to nanopure water. To quality check the optode measurements, DO was also measured via Winkler titration at a subset of 13 stations. The Winkler titrations were completed following standard operating procedures using 125-mL iodine flask bottles that were carefully filled with sample without bubbles (Bos 2013). The Winkler samples were then spiked with 1-mL of manganese chloride and 1-mL of sodium iodide-sodium hydroxide solution for preservation until analysis (Bos 2013).

Bottom water DIC and pH samples were also taken from the Niskin bottle. The 4-mL glass DIC vials and the 9-mL LabCo exetainers used for pH were overflowed with a few mL of sample to ensure that there was little to no exposure to the atmosphere. Directly after the vials were filled, the DIC and pH samples were poisoned with 10µL and 40µL of saturated mercuric chloride solution respectively and were refrigerated until analysis. The remaining bottom water collected from the Niskin bottle was also used to fill reservoirs that replaced water in the flux cores upon sampling (described further in following section).

Flux Core Sampling

During the incubation period, two water samples from the cores were taken from the overlying water to be analyzed for nutrients, DIC, and pH. Overlying water samples were collected by connecting one valve on top of the flux core cap to the water reservoir and the other valve to a 60-mL syringe. Pulling on the syringe removed overlying water without exposing it to the atmosphere and the reservoir of near bottom water immediately replaced the water that was removed so that no air bubbles were introduced to the core. Although the introduced water from the reservoir could have influenced the concentration of solutes in the overlying water slightly (particularly for the cores with a low volume of overlying water), I introduced water only once at the beginning of the incubation period when the overlying water concentrations were similar to the bottom water. In addition, only ~35-mL, or approximately 5% of overlying water, was replaced during sampling. Due to timing of the sampling and the small exchange volume, minimal impacts would have been made to the concentration of the overlying water and the measured benthic fluxes.

Roberts and Elliot (2017) suggested that sound or vibrations can inhibit bioirrigation and bioturbation, both of which heavily influence the benthic fluxes observed. To remove this influence from the benthic flux measurements, on-board incubations were performed overnight after the research vessel had docked and the engines were quiet. Flux cores were sampled twice, once in the evening and once again the following morning. For the three stations where the cores were incubated in the cold room, samples were taken on a similar schedule to the on-board incubations.

Each 35-mL flux core water sample was then filtered through a 0.2-µm nylon filter into glass vials for DIC (4mL, with additional few mL for overflowing the vial), LabCo Exetainers for pH (9mL, with additional few ml for overflowing the vial), and 20-mL plastic scintillation vials for nutrients (8 to 10 mL). As with the bottom water samples, the DIC and pH samples were preserved with 10µL and 40µL of saturated mercuric chloride and were refrigerated until analysis. The nutrient samples were frozen until analysis.

PreSens optode spots affixed to the inside of the flux core tubes were used to measure DO concentrations in the cores non-invasively. These optode spots were calibrated using the same methods as the bottom water DO vials. During incubations, DO measurements were taken at the same time as the flux core water samples. When there was additional time available, supplementary DO measurements were taken not long after the core had been capped or the following day before the sediment was removed from the core.

Sample Analysis

I determined the concentration of nutrients (nitrate+nitrite, ammonium, silicate, and phosphate) in my flux core samples using a Unity Scientific SmartChem chemical analyzer with colorimetric methods described by Gordon et al. (1993). An Apollo SciTech DIC analyzer was used to measure DIC concentrations in the flux cores and bottom water samples using the method described by Cai and Wang (1998). I measured pH using the cresol purple method with a diode array spectrophotometer and jacketed cuvette, following similar methods to those in Clayton and Byrne (1993). TA and aragonite saturation state were calculated using CO2SYS (Pierrot et al. 2006) with equilibrium constants from Millero (2010), which are suitable for estuarine waters.

Both the flux core and bottom water DO optode measurements were corrected for bottom water salinity found at each station using PreSens Oxygen Calculator software. A small linear difference was found between the bottom water DO measurements made with the optode spots and the Winkler titrations. The optode bottom water DO concentrations were adjusted to match the Winkler titration using the linear regression between the measurements.

Flux Calculation

Benthic fluxes for each core were calculated by determining the change in concentration over the elapsed time between measurements (i.e. slope). Because fluxes were calculated from just two time points, I made the assumption that the change in concentration was linear. The pilot study completed for my research, as well as many other benthic flux surveys, have found linear changes in nutrients, DO, and DIC concentrations (e.g. Berelson et al. 2003), although a linear relationship is not always the case (e.g. Hammond et al. 1996). When multiple DO measurements were made, the relationship between DO concentration and time were found to be consistently linear. To account for differences in overlying water volume among cores, the change in concentration over time was then multiplied by the height of the water column in the core. I calculated the mean flux for each solute by averaging the fluxes from the two replicate cores at each station.

A total of 12 cores and their corresponding fluxes were removed from the dataset prior to analysis based on physical and geochemical conditions that were not representative of the *in situ* system. The criteria for removal were if air bubbles appeared in the head space, if overlying water was anoxic by the second sampling, and if there was a low volume of overlying water. The DO concentrations of the overlying water has a large influence on the sedimentary respiration pathways and geochemical reactions that occur, therefore not only influencing the DO fluxes, but many of the other fluxes measured as well (Burdige 2006). The introduction of air bubbles, likely due to an insecure seal between the lid and core tube, were found between the first and second sampling in six cores from Stns. 40016, 40006, 40019, 40025, 40010, and HCB003. Air bubbles can also be introduced through the dissolution of gases produced from sediments, but because I did not determine where the air bubbles were from, I removed them the dataset. Positive DO fluxes are very unlikely to happen when incubated in the dark and likely indicate contamination from an external source of oxygen. This was found in one core from Stn. 29 and it was removed from the dataset. The enclosed nature of the flux cores can occasionally cause anoxia (DO concentrations < ~45µM) in the overlying water. This experimentally introduced anoxia would not normally occur *in situ* because water would constantly be exchanged by currents and water flow. A core from Stn. 40022 and both cores from Stn. 3 became anoxic before the second sampling and were removed from the dataset for this reason. A low volume of overlying water (height of the column < 6 cm) visibly disturbed the sediment surface and suspended sediment particles. This external disturbance can cause alterations in the observed fluxes, partially due to the introduction of oxygen into areas that would not normally be exposed. For this reason one core from Stn. 265 and one core from Stn. 40027 were removed from the dataset.

Data Collected by WA Department of Ecology:

At the time of flux core collection, DOE’s MSMT collected data on various geochemical parameters and properties of station sediments. Some of these environmental variables describing site conditions were used to assess the variability of the fluxes measured. The data collected by the MSMT that were included in my analysis were bottom water salinity (measured by refractometer), sediment grain size, percent total organic carbon, and sediment organic carbon to nitrogen ratios (C:N). A description of sampling and analytical methods used to collect these data can be found in Dutch et al. (2018).

The Marine Waters Monitoring Team (MWMT), also at DOE, monitors water quality parameters in the Salish Sea monthly. To estimate denitrification rates for each station, I used the MWMT measurements of particulate C:N ratios from bottom water in 2017 and 2018. I also used bottom water nutrient concentrations (nitrate, nitrite, ammonium, silicate and phosphate) and density measurements collected by the MWMT in early spring 2018 to estimate sediment contribution to water column ecosystem function. The sampling protocols and analytical measurements used by the MWMT are described in detail in Bos et al. (2015) and Keyzers (2017).

Estimating Denitrification Rates

Denitrification rates (the sum of nitrate reduction and annamox) were estimated at each station using the average benthic DIC and DIN fluxes and the nearby bottom water particulate C:N ratios collected by the MWMT. First, a rough estimate of organic carbon residence time was calculated for each station so that I could determine the time span over which to average water column C:N ratios. To do this, I used sediment grain size to estimate sediment porosity by following the marine sediment grain size – porosity relationship presented in Burdige (2006). The station porosity was then multiplied by a particle density of 2.65 g/cm^3 to determine sediment bulk density (Burdige 2006, Hamilton 1976). Bulk density was then multiplied the percent organic carbon and an assumed depth of 3 cm (depth where a majority of organic carbon respiration occurs in the form of aerobic respiration and nitrate reduction), to determine to the mass of organic carbon respired per m^2. The time required for reactive carbon in the top 3 cm to be respired was estimated by dividing the mass organic carbon m^{-2} of sediment by the DIC flux.

The weighted average C:N ratio of organic carbon reaching the sediment was then estimated for the length of the organic carbon residence time. A weighted average was calculated by using the total organic carbon concentration present to account for differences in the magnitude of organic carbon reaching the sediments during different time periods. This is an estimate the C:N ratio of organic carbon that would have hit the seafloor and would have been present in the sediment during the time of sampling. In cases where the core collection and bottom water particulate stations were not directly overlapping, a nearby particulate station that followed the average flow of bottom water to the sediment station was chosen to represent the organic matter reaching the seafloor at the sediment station. The particulate stations ranged from 1 to 30km away from the sediment sampling stations. The particulate sampling was not always completed at each station every month and in those cases the weighted averages were averaged over the months that most closely matched the organic carbon residence time.

The weighted average C:N ratio for the organic carbon at the stations was then used to estimate the amount of DIN flux expected if no denitrification were taking place. This calculation was completed by dividing the average station DIC flux by the average C:N ratios found in the sediment. The difference between the expected DIN flux and the one measured is the estimated denitrification rate for the station:

$$(1)\ \textit{Denitrification Estimate (mmol } m^{-2}\ d^{-1}) = \frac{DIC\ flux}{Weighted\ average\ C{:}N\ ratio\ of\ sediment\ organic\ carbon} - DIN\ flux$$

While several assumptions were made to calculate these stoichiometric denitrification rates, this indirect method of estimating denitrification is comparable to direct measurement methods such as the acetylene block approach (Joye et al. 1996) and the measurement of nitrogen gas fluxes (Horak et al. 2013).

Statistical Analysis:

I used canonical redundancy analysis (RDA) to assess how the variance observed in the fluxes were driven by key environmental variables. In RDA, a principal components analysis (PCA) is constrained to canonical axes that built from linear combinations of explanatory variables fitted by a multiple linear regression (Legendre and Legendre 1998). All environmental variables were assessed for collinearity by using the variance inflation factor test (VIF). The final set of environmental variables included in the RDA were water column depth, bottom water temperature, bottom water salinity, bottom water DO, bottom water TA, sediment total organic carbon, total percentage of fine grained sediments, and sedimentary organic carbon to nitrogen ratios.

Ecosystem Contribution Calculations

I calculated the influence that sediments have on springtime water column biogeochemistry in Puget Sound basins using the benthic flux measurements and denitrification rate estimates. These calculations were only made in Puget Sound because of the availability of bottom water residence times. I calculated the height of the bottom water as the distance between the average water column depth and the average pycnocline collected in March and April 2018 by the MWMT. I used the average nutrient concentrations of bottom water in March and April 2018 also collected by MWMT, average basin depths estimates from Duxbury (1987), and bottom water residence times estimated by Babson et al. (2006) to calculate a bottom water supply rate of DIN:

$$(2)\quad \textit{DIN Bottom Water Supply Rate (mmol m}^{-2}\textit{ d}^{-1}\textit{)} = \frac{Average\ bottom\ water\ DIN\ concentration\ (uM)}{Bottom\ water\ depth\ (m) * Basin\ Residence\ Time\ (d)}$$

I then divided the average denitrification rate for the basin by the bottom water supply rate, to calculate the proportion of the DIN supply removed by denitrification.

Storage of phosphate in the sediment was estimated using a stoichiometric method similar to the estimation of denitrification rates. With the assumption that the organic carbon reaching the seafloor follows the Redfield ratio of 106 carbon atoms to 1 phosphorus atom, the resulting fluxes of DIC and phosphate due to respiration should correspond to this same ratio if all of the phosphorus is released back to the overlying water. When the phosphate flux is less than the expected Redfield ratio, I attributed this to the storage of phosphate in the sediment. To estimate rates of phosphate storage at each station, I divided the DIC flux by the Redfield ratio and then subtracted the phosphate flux. The percentage of the organic phosphorus supplied to the sediment that was stored was calculated by dividing the phosphorus storage rate by the expected phosphorus flux based on the Redfield ratio. The organic matter reaching the seafloor likely has carbon to phosphorus (C:P) ratios that are higher than Redfield due to the preferential respiration of nutrient filled, labile organic matter in the water column (Faul et al. 2005). Due to this discrepancy between actual and theoretical C:P ratios of organic matter, my calculations of phosphorus storage are upper estimates.

To quantify contribution of sediment oxygen uptake to total bottom water oxygen consumption, I used measurements of total bottom water DO removal rates reported in Christensen and Packard (1976). These measurements were made in July through September 1972 in Dabob Bay, Hood Canal. I applied these rates to all the basins in Puget Sound due to lack of more recent and spatially relevant data. With Christensen and Packard’s data, I estimated the total DO removal occurring in the bottom water for each basin (both sediment uptake and water column respiration). The percentage of DO removal due to sediments was then calculated using the DO measured fluxes.

Results:

Benthic Flux Ranges and Spatial Patterns

Benthic fluxes varied considerably throughout the Salish Sea in the springtime (Table 1, Figure 3). In general, fluxes with relatively smaller magnitudes were found in the deep regions of the Central Basin and Hood Canal, whereas the larger magnitude fluxes were observed in shallow bays and terminal inlets, particularly in the Strait of Georgia (Figure 4 – 11). Although, this general trend had exceptions. High variability in benthic fluxes was also observed at the scale of the core replicates taken at each station. This variability introduced large standard errors associated with the average flux measurements and relative standard deviations (RSD) that were greater than 100% in some cases.

Fluxes of DO directed into the sediment ranged from -5.22 mmol m^{-2} d^{-1} (Stn. 281, Commencement Bay) to -38.22 (Stn. 40013, Lopez Sound) and the median was -11.78 mmol m^{-2} d^{-1} (Table 1, Figure 3). The median RSD for the DO fluxes for the two replicate cores from each station was 9%, which was the lowest observed out all the fluxes measured. Many of the shallow bays and inlets sampled had elevated oxygen fluxes, including Budd Inlet (Stn. 49), Sinclair Inlet (Stn. 34 and 40030), Port Orchard Bay (Stn. 40022), Port Angeles (Stn. 40005), Lopez Sound (Stn. 40013), West Sound near Orcas Island (Stn. 40025), Bellingham Bay (Stn. 40029 and 4), Birch Bay (Stn. 40009), and Boundary Bay (Stn. 40017) (Figure 4). These last five stations were all located in the northern portion of the study area in the Strait of Georgia. Unlike many of the other bays and inlets, Carr Inlet and Case Inlet in the South Basin of Puget Sound did not have elevated DO fluxes. In general, the lowest DO fluxes in the spatial survey were located in the deep regions of the Central Basin and Hood Canal.

The DIC fluxes ranged from -1.10 mmol m^{-2} d^{-1} (Stn. 52, Anderson Island) to 34.31 mmol m^{-2} d^{-1} (Stn. 40013, Lopez Sound) and the median value was 6.65 mmol m^{-2} d^{-1} (Table 1, Figure 3). The unexpected measurement of an average DIC flux into the sediment was only found at Stn. 52 near Anderson Island in the South Basin, although a few locations had fluxes that were very close to zero, such as West Sound, Orcas Island (Stn. 40025) and Sinclair Inlet (Stn. 34). The median RSD for the DIC fluxes in replicate cores was 31%. This variability may have contributed to the negative DIC fluxes observed. The stations that had very elevated DIC fluxes (outliers in boxplot) were Stn. 40018 (South Hood Canal), Stn. 40013 (Lopez Sound) and Stn. 40029 (Bellingham Bay). Similar to the spatial pattern in the DO fluxes, many of the low DIC fluxes were found in the deep stations in Central Basin and Hood Canal (Figure 5).

The hydrogen ion flux, calculated from the change in pH in the flux cores, is primarily composed of free hydrogen ions with a small contribution from hydrogen sulfide ions (HSO_4^-) (Clayton and Byrne 1993). A majority of the hydrogen ion fluxes measured had a net output of hydrogen ions into overlying water (Table 1). The hydrogen ion fluxes ranged from -0.18 µmol m^{-2} d^{-1} (Stn. 40015, Whidbey Basin) to 1.28 µmol m^{-2} d^{-1} (Stn. 40005, Port Angeles) with a median value of 1.28 µmol m^{-2} d^{-1} (Figure 3). The median RSD for the hydrogen ion fluxes in replicate cores was 24%. The two fluxes that had a slight reduction in hydrogen ions (increased in pH) over the incubation period were Stn. 40015 in West Sound, Orcas Island and Stn. 29 in the middle of the Main Basin (Figure 6). The large effluxes of hydrogen ions where flux core water became more acidic were generally found in stations in the South Basin (Stns. 49, 40028, 52, 265), as well as Lopez Sound (Stn. 40013) and Whidbey Basin (Stn. 40021, 40007, 40015).

The springtime TA fluxes in the Salish Sea included both a net uptake of alkalinity into the sediment and a net release from the sediment into the overlying water (Table 1, Figure 3).

The TA fluxes, which were calculated from the DIC and pH in flux cores samples, ranged from -13.10 mmol m^{-2} d^{-1} (Stn. 52, Nisqually Reach) to 29.38 mmol m^{-2} d^{-1} (Stn. 40018, South Hood Canal). The median flux was 1.26 mmol m^{-2} d^{-1}. The stations with high DIC fluxes generally had elevated TA fluxes as well, due to bicarbonate and carbonate being important contributors to alkalinity. The RSD associated with the TA fluxes was higher than the DIC and hydrogen ion fluxes, with a median value of 88%. This was the largest median RSD in the dataset. The TA fluxes in Hood Canal and Bellingham Bay were all positive fluxes indicating a net release of alkalinity into the overlying water (Figure 7). At stations in the Central, South, and Whidbey Basins, a mixture of both negative and positive fluxes were observed.

Ammonium was both released and taken up by the sediments during the springtime (Table 1). The range of ammonium fluxes were from -0.40 mmol m^{-2} d^{-1} (Stn. 252, Carr Inlet) to 1.23 mmol m^{-2} d^{-1} (Stn. 40022, Port Orchard Bay), with a median flux of 0.10 mmol m^{-2} d^{-1} (Figure 3). The median RSD for the ammonium fluxes was comparable to the RSD for the TA fluxes at 84%. The stations with elevated fluxes generally had a higher degree of variability between the replicate measurements. Hood Canal and deep Central Basin stations generally had uptake or a low efflux of ammonium (Figure 8). Stations in the South Basin varied considerably with high fluxes in Budd Inlet (Stn. 49), Totten Inlet (Stn. 40028), and Carr Inlet (Stns. 265 and 40008) and very low fluxes in Case Inlet (Stns. 252 and 40032). The stations with the highest ammonium fluxes were found scattered throughout the Salish Sea, in Sinclair Inlet (Stn. 40030), Port Orchard Bay (Stn. 40022), Possession Sound (Stn. 40019), Oak Harbor (Stn. 40021), Bellingham Bay (Stn. 40029), and Port Angeles (Stn. 40005).

Nitrate+nitrite fluxes ranged from -1.94 mmol m^{-2} d^{-1} (Stn. 40013, Lopez Sound) to 0.01 mmol m^{-2} d^{-1} (Stn. 281, Commencement Bay) and the median flux was -.34 mmol m^{-2} d^{-1} (Table

1, Figure 3). The median RSD for the average nitrate+nitrite fluxes was 49%. All but two stations, Stn. 40020 in the Central Basin and Stn. 281 in Commencement Bay, had sedimentary nitrate+nitrite uptake. Considering the standard error and variability range, both of these fluxes were not different than zero. Stations in the deep regions of the Central Basin had nitrate+nitrite fluxes that were distinctly lower than other regions in the Salish Sea (Figure 9). High nitrate+nitrite uptake was found in many stations in the northern regions of the Salish Sea, like Bellingham Bay (Stns. 4 and 40029), Lopez Sound (Stn. 40013), and Port Angeles (Stn. 40005). Whidbey Basin (Stns. 40019, 40037, and 40021) and Port Orchard Bay (Stn. 40022) also had above average nitrate+nitrite fluxes.

Silicate fluxes had a considerably large range with both negative and positive fluxes (Table 1, Figure 3). The lowest silicate flux was -1.16 mmol m^{-2} d^{-1} (Stn. 49, Budd Inlet), while the highest was 20.29 mmol m^{-2} d^{-1} (Stn. 40029, Bellingham Bay). The median silicate flux was 5.34 mmol m^{-2} d^{-1}. Only two stations had negative silicate fluxes: Stn. 281 in Commencement Bay and Stn. 49 in Budd Inlet. Both of these stations' standard errors were fairly large and the variability indicates that these fluxes were not different from zero. The silicate fluxes had a median RSD of 33%. Saratoga Passage in Whidbey Basin (Stns. 40021 and 40015), Bellingham Bay (Stns. 40029 and 4), Port Angeles (Stn. 40005), and Lopez Sound (Stn. 40013) all had elevated silicate fluxes greater than 12 mmol m^{-2} d^{-1} (Figure 10). Mid-range silicate fluxes were found in the deep stations of the Central Basin and were remarkably similar throughout (Stns. 38, 191, 40006, 40038, 29, 40020, and 40011). The lowest silicate fluxes were found in most of the South Basin inlets (excluding Carr Inlet, Stns. 40028, 49, 40016, 52, and 40032), Sinclair Inlet (Stns. 34 and 40030), and Commencement Bay (Stn. 281).

Springtime phosphate fluxes had a very small range from -0.17 mmol m^{-2} d^{-1} (Stn. 40013, Lopez Sound) to 0.06 mmol m^{-2} d^{-1} (Stn. 40020, mid-Central Basin) (Table 1, Figure 3). The median flux was -0.01 mmol m^{-2} d^{-1}. A total of 12 stations had standard errors greater than the fluxes, making them indifferentiable from zero. The median RSD for the phosphate fluxes was also fairly high at 69%. All of South Basin had average fluxes that were negative, whereas Saratoga Passage in Whidbey Basin generally had positive phosphate fluxes (Figure 11). Due to the small range of uptake or release of phosphate and the variability observed between replicates, the phosphate fluxes were not included in the canonical redundancy analysis.

Some stations in the survey repeatedly had fluxes that were outliers in the dataset. Lopez Sound (Stn. 40013) had DO, DIC , nitrate+nitrite, and phosphate fluxes that were all larger than the 1.5 interquartile range of the flux distributions (Figure 3). Stn. 40029 in Bellingham Bay also had DIC, TA, and silicate fluxes that were high outliers in the dataset. Stn. 40018 in south Hood Canal also had large outlying DIC and TA fluxes. While never outliers, the fluxes measured in Port Angeles harbor (Stn. 40005) were large in magnitude for all but the TA flux.

Denitrification Rate Estimates

Ratios of benthic fluxes can be used to infer various biogeochemical processes occurring in the sediments, particularly when the molar ratios deviate from expected values. Due to respiration in the sediments, the expected ratio of the DIN to DIC fluxes (DIN:DIC) is the N:C ratio of the organic matter reaching the seafloor (Giblin et al. 1997, Joye et al. 1996). The weighted average for N:C ratios of near bottom organic matter from April 2017 – 2018 across the Salish Sea was 0.10. A majority of the stations had DIN:DIC fluxes that fell below the expected 0.10 N:C ratio of the organic matter reaching the seafloor (Figure 12a). I attribute the reduced flux of DIN relative to DIC to the conversion of DIN into nitrogen gas through denitrification. With the exception of one outlier, the DIN fluxes stayed within a -0.5 to 0.5 mmol m^{-2} d^{-1} band across the range of DIC fluxes measured.

Denitrification rates were estimated for all of the stations using the deviation from the expected N:C ratios. Denitrification rates ranged from close to zero (Stn. 40025, West Sound, Orcas Island) to 4.07 mmol m^{-2} d^{-1} (Stn. 40013, Lopez Sound). Interestingly, these maximum and minimum denitrification rates were both located in the San Juan Islands. Although the two stations were close in proximity, they had very different sediment biogeochemistries. The median estimated denitrification rate was 1.05 mmol m^{-2} d^{-1} (Table 1). Lopez Sound (Stn. 40013), south Hood Canal (Stn. 40018), and all of the stations in Bellingham Bay (Stns. BLL009, 4, and 40024) had the highest estimated denitrification rates (Figure 13). West Sound Orcas Island (Stn. 40025) and Everett harbor (Stn. 40019) had low or negative estimated denitrification rates. The negative estimates of denitrification can be caused by nitrogen fixation, or more likely reflects the uncertainty in the fluxes or N:C ratios of organic matter hitting the seafloor. Most areas in the Salish Sea had estimated denitrification rates that ranged between 1 and 2 mmol m^{-2} d^{-1}.

Phosphorous Storage

Similar to the DIN:DIC fluxes, the phosphate to DIC fluxes (P:DIC) fluxes would be expected to follow the ratio of phosphorus to carbon (P:C) of the organic matter settling on the seafloor. Although no P:C measurements were made or were available of the near bottom organic matter, it is informative to compare the fluxes to the Redfield ratio (P:C=0.009) to determine the fate of phosphorus in the sediment. Since nitrogen is the limiting nutrient in the Salish Sea, it is likely that the organic matter has P:C ratios close to Redfield in the surface (Nakata and Newton 2000). Yet, as organic matter particles sink through the water column respiration occurs and the P:C ratios of organic matter likely increase, which make my estimates based on the Redfield ratio the upper limits of storage rates. During the springtime, Salish Sea sediments had P:DIC flux ratios that followed the Redfield ratio or were below it (Figure 12b). The low phosphate flux relative to the DIC flux indicates that the phosphorus originating from organic matter had net storage in the sediment. The phosphate fluxes were generally located within the same range above or below zero, and were not dependent on the magnitude of the DIC fluxes (Figure 12b).

Oxidation of Reduced Compounds

Comparing the DO flux to the DIC flux, which is the best estimate of total respiration occurring in the sediments, can inform whether the reduced byproducts of anaerobic respiration are stored (DO flux ≤ DIC flux relationship) or whether previously stored reduced compounds are oxidized (DO flux > DIC flux; Giblin et al. 1997). A majority of the stations (32 out of the 41 with DIC fluxes) had DO fluxes that were greater than the DIC flux (Figure 12c). The stations with the highest DIC fluxes (> 12 mmol m^{-2} d^{-1}), generally had DO fluxes that were less than the 1:1 relationship. This indicates that stations with lower respiration rates had DO fluxes that were driven by the oxidation of stored reduced by products of anaerobic respiration, while the stations with high respirations rates were storing reduced byproducts.

Canonical Redundancy Analysis

I used canonical redundancy analysis (RDA) to determine which environmental variables best explained the variation observed in benthic fluxes and denitrification rates. Stations 34, 40007, 40009, 40017, and 209R were removed from the RDA because they did not have corresponding bottom water DO, DIC, or pH data. To make the analysis easier to interpret, the DO flux was represented as a negative flux representing DO uptake into the sediment. The RDA model with

32 stations and eight environmental variables explained 35% of the total variance observed in the fluxes and estimated denitrification rates, with the first and second axis explaining 22% and 8% respectively. The complete RDA model was determined to be significantly different than 999 randomized versions ($F_{8,27}$ = 1.78, p-value = 0.042), but the seven individual RDA axes were not significantly different than the randomized axes. While the RDA did not explain a majority of the variation, informative relationships between fluxes and environmental variables were nevertheless apparent.

The first RDA axis was primarily driven by water column depth and separated the shallow and deep sampling stations along the x-axis (Figure 14). The shallower stations had larger flux magnitudes indicated by many of the flux vectors pointing in the opposite direction of depth vector (Figure 14). The second RDA axis was driven by bottom water DO and TA concentrations. Stations did not cluster together based on major water body or basin in the ordination (Figure 14). Stations within the same inlet were not always positioned close to one another either. This suggests that neighboring stations did not necessarily have similar benthic fluxes and sediment biogeochemistry. Instead the variation in benthic fluxes were driven by water column depth and bottom water DO, which were not necessarily associated with the broader water body.

Interesting patterns among fluxes can also be observed in the ordination. Correlations are indicated by vectors pointing in the same or opposite directions. Yet, because the data are multidimensional and are projected onto a two-dimensional plane, it can sometimes lead to vectors that are linearly oriented without any correlation. Therefore, Kendall’s rank correlation test was used to test the significance of relationships among variables found in the ordination.

The DIC flux, representative of organic matter breakdown and calcium carbonate dissolution/precipitation, is correlated with the silicate flux ($\tau = 0.49$, $p < 0.001$; Figure 14). As indicated by the opposing orientation, the nitrate+nitrite flux (uptake into the sediment) is also weakly correlated with the DIC flux ($\tau = -0.26$, $p = 0.02$). It is important to note that the estimated denitrification rates were calculated using the DIC and DIN fluxes and the C:N ratio of the organic matter in the bottom water. Because the estimated denitrification rates were not independent of the DIC and DIN fluxes, I did not perform a significance test.

The DO uptake was highly correlated with both the ammonium flux ($\tau = -0.41$, $p < 0.001$) and the hydrogen ion flux out of the sediment ($\tau = 0.47$, $p < 0.001$). Interestingly, DO uptake was correlated with the DIC flux ($\tau = 0.26$, $p = 0.02$), but this was not apparent in the plot. Bottom water DO concentration, driver of the second RDA axis, and the DO uptake vectors were aligned and better correlated ($\tau = 0.38$, $p < 0.001$).

Sediment Contribution to Water Column Biogeochemistry

To quantify the role that sediments play in water column biogeochemistry in the springtime, I estimated the contribution that sediment fluxes make to changes in water column chemistry of Puget Sound basins (Table 3). It is important to note that these are estimates for springtime sediment-water column relationships and should not be extrapolated to an annual timescale due to expected seasonal variability.

The influence of denitrification on bottom water chemistry was determined by calculating the supply rate of DIN to the bottom water based on average DIN concentrations, bottom water depth, and residence time for the basin. The percentage of the DIN supply that was removed from the water column via denitrification ranged from 1.2% in the Central Basin to 10.9% in Hood Canal (Table 3).

The percentage of particulate phosphate stored in the sediments was calculated for each station based on the ratio of the estimated rate of phosphorus storage and the expected flux of phosphorus based on the Redfield ratio. Because phosphorus fluxes were so low compared to the estimated rate of organic P supply, essentially all of the particulate organic phosphate supplied to seafloor was stored in the sediments during the springtime (Table 3). An additional 10 – 30% more inorganic phosphorus was removed from the bottom water in the South, Whidbey, and Central Basins. There was high variability associated with the basin average storage rates demonstrating the variability among stations (Table 3).

For each basin, I compared the benthic fluxes of DO to the total bottom water DO removal rates measured by Christensen and Packard (1976) and then determined the percentage due to the sediment uptake. The percentage of bottom water DO removal due to the sediments ranged from 21 to 35%, but in the South Basin this percentage was equal to 80% (Table 3). Based on my calculations for DIN removal, phosphate storage, and DO uptake, the sediment in the Central Basin generally had the smallest influence on bottom water chemistry, whereas benthic fluxes in the South Basin had the largest.

Discussion:

This study is the first broad spatial analysis of benthic DO, DIC, pH, TA, and nutrient fluxes in the Salish Sea. These benthic fluxes exhibit large variability across several scales from the 100-km scale of the basins, the 10-km scale of inlets, down to the 10-m scale of replicate core samples.

Benthic Flux Comparisons

The benthic fluxes measured in my study fell within the ranges of previous benthic flux measurements completed in the Salish Sea, although there were some discrepancies (Belley et al. 2016, Pamatmat 1971, Sheibley and Paulson 2014). The springtime DO fluxes measured in my study were higher than measurements made by Pamatmat (1971), but correspond to well to those made by Belley et al. 2016. The average basin DO fluxes from my study were 1.6 (Central Basin) to 3.4 (Whidbey Basin) times larger than the average annual values presented by Pamatmat (1971). Those benthic fluxes were averaged over the entire year and encompassed seasonal changes, which could be why the values differ.

Sheibley and Paulson (2014) compiled all available data on benthic nitrogen fluxes in Puget Sound. The median nitrate+nitrite flux measured in this study, -0.34 mmol m^{-2} d^{-1} , was slightly lower than the results reported by Sheibley and Paulson (-0.68 mmol m^{-2} d^{-1}). A larger difference was found between the ammonium fluxes. This study observed a median ammonium flux of 0.10 mmol m^{-2} d^{-1} whereas Sheibley and Paulson found a median value of 1.8 mmol m^{-2} d^{-1}. Similar to Pamatmat (1971), the medians from Sheibley and Paulson were compiled into yearly datasets. From the few seasonal analyses of Puget Sound benthic fluxes of nitrogen, Sheibley and Paulson found that ammonium fluxes were lowest in the spring (~ -0.9 mmol m^{-2} d^{-}

^{1} to ~1.4mmol mmol m^{-2} d^{-1}) and highest during the late summer to early fall (~1.4 mmol m^{-2} d^{-1} to 13.5 mmol m^{-2} d^{-1}), which could explain the large discrepancy in ammonium fluxes.

The most recent study on benthic fluxes in the Salish Sea was completed by Belley et al. (2016), who measured DO and nutrient fluxes in the western region of the Strait of Georgia near Vancouver Island. The median DO flux measured by Belley et al. in May 2015 was -8.9 mmol m^{-2} d^{-1}, which was ~2.9 mmol m^{-2} d^{-1} lower than the median flux observed in my study. The difference in average oxygen uptake could be due to fewer stations in the study by Belley et al. And, although the environmental variables were not reported, they might have measured fluxes with different water column depths and bottom water DO concentrations than this study. The median ammonium (0.18 mmol m^{-2} d^{-1}), nitrate+nitrite (-0.36 mmol m^{-2} d^{-1}), and silicate (4.32 mmol m^{-2} d^{-1}) fluxes measured by Belley et al. were only ± 0.5 mmol m^{-2} d^{-1} different than those measured in this study. Belley et al. also measured phosphate fluxes that were continuously low, but were only released from the sediment. This contrasts with my observations of primarily negative phosphate fluxes.

Benthic fluxes of DIC, hydrogen ions, and TA have never been reported in the Salish Sea, so the following benthic flux comparisons were made with other estuaries. In general, the DIC fluxes measured in the Salish Sea were less than those measured in San Francisco Bay (Hammond et al. 1985), Tomales Bay (Dollar et al. 1991), and Boston Harbor (Giblin et al. 1997) during the winter to spring months. The average *in situ* DIC fluxes measured in the afore mentioned locations ranged from ~10 to 70 , compared to ~ -1 to 34 measured in my study, with the greatest difference occurring in Boston Harbor. One particular difference between these estuaries and the Salish Sea that could be driving this large deviation is that these stations were relatively shallow with a maximum depth of 19 m compared to a max depth of 203 m in the

Salish Sea stations. Although, the Salish Sea stations with an average depth less than 25m had a median flux of 7.1 mmol m^{-2} d^{-1}, which is still lower than the other estuaries. The DIC fluxes measured in the Salish Sea also had a much greater range of DIC fluxes compared to the other locations, which could be due to large spatial area and various depths sampled in my study.

The TA fluxes measured in the Salish Sea were much more variable compared to those measured in San Francisco Bay (Hammond et al. 1985) and Tomales Bay (Dollar et al. 1991) in the winter to spring. The lowest average TA fluxes in these studies were found in San Francisco Bay at -1.1 mmol m^{-2} d^{-1} (Hammond et al. 1985), compared to -13.10 mmol m^{-2} d^{-1} in the Salish Sea. The highest TA flux in the Salish Sea, 29.38 mmol m^{-2} d^{-1} was more than double the highest found in Tomales Bay (11.64 m^{-2} d^{-1}; Dollar et al. 1991). Despite these differences, the median TA flux of 1.26 mmol m^{-2} d^{-1} in the Salish Sea was comparable to that measured in San Francisco Bay. In my study, the core replicates also had highly variable TA fluxes within a station. This large range of TA fluxes observed in the Salish Sea was likely due to small-scale physical, chemical, and biological differences among stations and replicates.

The release of TA from the sediment was likely influenced by higher rates of anaerobic respiration (high release of DIC), whereas the negative TA fluxes were likely driven by higher rates of stored reduced compounds being oxidized (high DO uptake and high release of hydrogen ions; Burdige 2006). Positive TA fluxes were found at the nine stations where DIC fluxes were greater than DO fluxes. At these stations, anaerobic respiration contributed to a high DIC efflux and release of TA. All of the stations with negative TA fluxes had DO fluxes that were greater than the expected 1:1 ratio, inferring that stored reduced compounds were being oxidized. The hydrogen ions produced from these oxidation reactions led to lowered TA in the overlying water. Biogenic calcium carbonate precipitation could have also led to TA uptake. Green and Aller

(2001) found strong seasonal patterns associated with TA fluxes, especially in the springtime due to the recruitment of shell-bearing benthic organisms. Whereas my incubated cores were small in diameter, some small, newly recruited calcifiers may have been included in the samples and influenced the DIC and TA fluxes.

While hydrogen ion fluxes into the overlying water were small, it is important to consider the impacts that they may have throughout the year as respiration rates change and how they may contribute to ecosystem-scale acidification. Lowe et al. (2019) found that biological production and metabolism drives the seasonal variability in pH and has accelerated the pH decline in the Salish Sea over the past 25 years. Thus, it is critical to quantify all components of the hydrogen ion budget in the Salish Sea.

Overall, previous studies completed in the Salish Sea and other estuaries were consistent with the benthic fluxes measured in my study. This is despite the highly variable benthic fluxes measured between core replicates. Three possibilities could explain this variation between core replicates: sample contamination, analytical error, or highly patchy sample sites. The samples of seawater taken to calculate the fluxes were carefully removed from the cores with syringes previously rinsed with sample, sample vials were immediately filled, and for DIC and pH, the samples were spiked with mercuric chloride quickly all to prevent atmospheric exposure. These precautions makes it unlikely that sample contamination occurred at time of collection. The samples were stored for approximately two months before analysis, which could be a potential factor in the error associated with the measurements. Baseline and sample drift on the instruments were not observed throughout the sample runs and all of the standard curves were linear with $R^2 > 0.99$. While the cores were sampled on average only 7.5m away from one another at each sampling site, it is more likely that sediment properties varied among replicate samples and drove the variability in the fluxes. The patchiness within sites is likely due to variation in organic matter availability, microbial activity, or benthic infaunal activity in the sediments. These components all drive benthic fluxes, yet can vary on the scale of meters.

Other studies in the Salish Sea have also observed this high variability on small spatial scales (Belley et al. 2016, Sheibley and Paulson 2014). The median RSD's associated with the average benthic measurements from replicate cores in Belley et al. (2016) were also considerably high. The median RSD's for the benthic fluxes of ammonium (105%), nitrite (107%), nitrate (63%), silicate (48%), and DO (20%) reported by Belley et al. were all higher than those in my study by at least 10%. The phosphate flux median RSD was lower in Belley at al. (54%) than in my study (69%). Similar high variability in DIN fluxes were also found on the scale of ~20 km^2 in Budd Inlet located in the South Basin (Sheibley and Paulson 2014). Both the support from previous studies in the region and the precautions taken in sample collection and analysis, lead to the conclusion that the variation observed in replicate cores were due to small-scale spatial variation in sediment biogeochemistry.

Spatial Variation and Environmental Drivers

Springtime benthic fluxes varied considerably across the study region. Stations did not group by general waterbody and, occasionally, not even by inlet (Figure 14). The RDA ordination supports the conclusion that spatial heterogeneity in the Salish Sea is high and is not primarily driven by differences among basins.

The principal environmental variables driving the variation in benthic fluxes between stations was water column depth and bottom water DO. The depth of the water column influences the amount of organic carbon reaching the sediments (Burdige 2006). In deeper stations, more water column respiration can occur, reducing the rain and the quality of organic matter to the seafloor. Thus, shallow stations generally receive more reactive organic matter, leading to higher rates of respiration and benthic fluxes (Burdige 2006).

Belley et al. (2016) noted the importance of water column depth in Salish Sea nutrient fluxes, but considered the main environmental driver of benthic fluxes to be bottom water temperature. In the Salish Sea, water depth and temperature are correlated. The temperature of sediments can influence the rates of respiration, which often produces confounding affects making it difficult tease these apart (Burdige 2006). Given that both water depth and bottom water temperature were included in my RDA, it was clear that depth was the stronger explanatory variable for the springtime fluxes measured in the Salish Sea due to its strong correlation with the first RDA axis (Figure 14).

Bottom water DO concentration was the other main environmental variable driving the variation in the observed benthic fluxes. The concentration of DO in bottom water strongly influences both bottom water and sediment geochemistry. Oxygen availability influences the types of sedimentary respiration that can occur (aerobic vs. anaerobic) and the geochemical reactions that take place (Burdige 2006, Middelburg and Levin 2009). Fluxes across the sediment-water interface are partially due to a diffusive gradient between the sediment and the overlying water. Low concentration of bottom-water oxygen results in a small diffusive gradient and would reduce the DO flux. In Hood Canal, where I observed the lowest bottom water DO concentrations, I also observed some of the lowest DO fluxes. Low bottom water DO has been previously found to cause elevated ammonium fluxes due to decreased rates nitrification (Middelburg and Levin 2009). This trend was also observed in my study, as indicated by the bottom water DO and ammonium flux vector pointing in the same direction in the RDA ordination (Figure 14).

The correlation between the DIC and silicate fluxes is understandable given the taxonomic composition of phytoplankton in the Salish Sea. Diatoms are generally the most abundant phytoplankton taxon in the open waters in the Salish Sea, which were where the silicate fluxes were the greatest (Strickland 1983, Figure 9). The stratified inlets, that commonly support higher flagellate populations (Strickland 1983), had lower silicate fluxes. The silicate flux is likely a natural consequence of the breakdown of diatom silicate frustules following burial and is consistent with other observations in benthic flux studies (Berelson et al. 2003, Berelson et al. 2019).

The DO and DIC fluxes were weakly correlated, but were not linearly oriented in the ordination (Figure 14). Additionally, the DO fluxes were on average 1.3 times greater than the DIC fluxes (Figure 12c). The weak correlation and relatively higher DO fluxes suggests that the DO flux was not only driven by sedimentary respiration. It was also caused by the oxidation of reduced compounds produced from previous anaerobic respiration. This relationship was also supported by the very high correlation between the DO and hydrogen ion fluxes (Figure 14). Oxidation of reduced compounds, such as sulfide, releases hydrogen ions, which can then be released from the sediment. The reduced compounds were likely produced from anaerobic respiration that occurred during time periods of low oxygen and high organic carbon deposition, such as weeks following the spring bloom. Then the compounds were likely slowly oxidized during winter and early spring, although seasonal measurements would be necessary to assess this.

Unexpectedly, I observed a high correlation between DO and ammonium fluxes (Figure 14). Ammonium fluxes are usually a function of organic matter breakdown in the sediment (Nixon 1981), but if DO fluxes were primarily due to the oxidation of reduced compounds as previously suggested, it was surprising that the ammonium flux was so highly correlated. One process that could have potentially influenced the ammonium flux from the sediments was dissimilatory nitrate reduction to ammonium (DNRA). This microbial pathway converts nitrate to ammonium via heterotrophic respiration and autotrophic production of organic matter (Giblin et al. 2013). The autotrophic DNRA pathway utilizes nitrate to oxidize reduced inorganic compounds, such as sulfides (Giblin et al. 2013). If DO fluxes were primarily driven by the oxidation of reduced compounds, it is expected that those same reduced compounds could be utilized by microbes operating with the autotrophic DNRA pathway. Additionally, a correlation between high DO uptake and DNRA rates has been previously found in a fjord environment similar to the Salish Sea (Christensen et al. 2000). Enhanced DNRA could be a potential cause for the correlation, but multiple types of microbial activities could have influenced the ammonium flux (e.g. anammox, nitrification) and with the data collected, it is difficult to specify the direct influence from each component. To determine and constrain the variables controlling the relationship between the ammonium and DO fluxes, more detailed measurements need to be made on the nitrogen cycle in the Salish Sea.

Sediment Contribution to Water Column Biogeochemistry

The estimates for sediment contribution to bottom water biogeochemistry also varied between Puget Sound basins. The largest sediment contributions to bottom water biogeochemistry occurred in Hood Canal and the South Basin, whereas the lowest contribution was found in the Central Basin (Table 3). Basin characteristics, particularly bottom water residence time and water depth, were the main factors that controlled the amount of influence sediments had on water column biogeochemistry.

Hood Canal was found to remove ten times the bottom water DIN through denitrification compared to other basins (Table 3). In contrast, the Central Basin had the lowest DIN removal due to denitrification. While the Central Basin and Hood Canal had the deepest average depths, the long bottom water residence time in Hood Canal (~88 days, Babson 2006) allows the sediments to remove more DIN before the bottom water is exchanged. Other studies have also found that low bottom water DO concentrations can lead to increased denitrification rates (Berelson et al. 1996, Cornwell et al. 1999, Middelburg et al. 1996), which is another distinguishing characteristic of Hood Canal (Newton et al. 2007).

Based on the calculations I made which assumed that C and P in settling organic matter were in Redfield proportions, nearly all of the particulate organic phosphorus sinking to the seafloor was stored in the sediments (Table 3). In the South, Central, and Whidbey basins, an additional 10 – 30% of this supply of phosphorus was also removed from bottom water. During periods of low surface productivity, like the early spring, there is less of a biological demand for oxygen which makes the sediments relatively oxic. The presence of oxygen in the sediments encourages the binding of phosphate to iron (Burdige 2006), which is likely the driving force behind the uptake of bottom water phosphorus. Although, this iron-bound phosphorus is not necessarily permanently stored because it can be released back to the overlying water during low oxygen conditions (Burdige 2006).

Based on my estimates, the South Basin had the highest percentage of bottom water DO removal caused by the sediments (80%, Table 3). The shallow average depth of the South Basin and the elevated DO fluxes led to this high estimate of sediment oxygen uptake. The South Basin is the shallowest basin in Puget Sound at an average depth of 45m (Duxbury 1987). Shallow coastal areas can have strong pelagic-benthic coupling due to the high export of organic matter to the sediments, which enhances sedimentary respiration (Burdige 2006). Some of the sedimentary DO uptake is due to respiration, as well as a portion due to the oxidization of reduced compounds stored in the sediments. Although shallow water depth was the main reason for the importance of South Basin sediments in terms of bottom water DO removal, the high DO fluxes in this location suggest that there may be higher levels of organic matter or high concentrations of reduced sulfide or iron. To test this concept, sediment biogeochemistry should be measured across seasons in the South Basin.

These estimates of sedimentary contribution to water column biogeochemistry illuminate the important role that coastal sediments play in Puget Sound basins during the springtime. Larger sedimentary influences were found in basins with shallow water column depths and long residence times. In order to understand the ecosystem contribution of sediments across seasons, future work should be focused on measuring the seasonal variation of benthic fluxes across the Salish Sea. This type of future research would continue to develop the understanding of the role that sediments play in the broader ecosystem biogeochemistry, as well as inform critical ecosystem models.

Conclusion:

Our spatial survey of springtime benthic fluxes of DO, DIC, pH, TA and nutrients in the Salish Sea indicated high variability across the region. We found that station fluxes did not correspond to station basin or waterbody, indicating that the basin wide dynamics were not driving the fluxes. Water column depth and bottom water DO concentrations were the two environmental variables driving the greatest amount of variation found in the fluxes.

We also calculated estimates of sediment contribution to water column biogeochemistry in Puget Sound basins using measured benthic fluxes and bottom water properties. Hood Canal exhibited a relatively high removal of DIN via denitrification due to the long residence time, whereas the South Basin had high sedimentary DO removal due to the shallow water column depth. Nearly all of the particulate phosphate supplied to the seafloor was estimated to be stored in the sediments during the springtime. This study suggests that it is important to consider sedimentary contribution to water column biogeochemistry in waterbodies with high residence times and that are shallow. Future work should be completed on the seasonal variation of benthic fluxes in the Salish Sea.

Table 1. Springtime benthic fluxes and estimated denitrification rates (removal of DIN via nitrate reduction + anammox) measured in mmol m^{-2} d^{-1} and hydrogen ion fluxes reported in µmol m^{-2} d^{-1}. Standard error is included in parentheses. If no standard error is included, only one core was successfully collected and sampled. Bolded values indicate fluxes that have standard errors larger than the flux.

Station	Dissolved Oxygen (DO)	Dissolved Inorganic Carbon (DIC)	Hydrogen ion (H^+)	Total Alkalinity (TA)	Ammonium (NH_4^+)	Nitrate +Nitrite (NO_3^-+$NO_2^=$)	Silicate (Si)	Phosphate (PO_4^3)	Estimated Denitrification
4	-16.59 (± 2.31)	12.89 (± 3.24)	0.76 (+/- 0.47)	5.73 (± 0.47)	0.21 (± 0.14)	-0.76 (± 0.27)	12.40 (± 0.11)	-0.08 (± 0.02)	2.23
13	-11.78 (± 1.36)	6.93 (± 0.80)	0.44 (+/- 0.03)	1.88 (± 0.17)	**0.10 (± 0.21)**	-0.04 (± 0.10)	7.16 (± 2.06)	-0.01 (± 0.03)	0.96
19	-9.17 (± 0.68)	**4.08 (± 8.87)**	0.57 (+/- 0.02)	**-0.21 (± 9.24)**	-0.01 (± 0.00)	-0.49 (± 0.04)	6.56 (± 0.11)	0.01 (± 0.04)	0.86
21	-6.71 (± 0.10)	**1.02 (± 20.68)**	0.23 (+/- 0.06)	**3.68 (± 12.14)**	0.11 (± 0.01)	-0.34 (± 0.12)	1.80 (± 0.38)	-0.02 (± 0.00)	0.31
29	-8.49	5.23	-0.04	5.80	-0.30	-0.31	4.19	0.01	1.22
34	-17.77 (± 0.96)	1.39	1.10	-12.01	0.00 (± 0.21)	-0.48(± 0.10)	3.38 (± 0.98)	0.01 (± 0.06)	0.66
38	-6.10	3.78	0.45	-0.90	-0.19	-0.21	5.57	0.01	0.81
49	-26.48 (± 2.16)	7.24 (± 5.54)	1.03 (+/- 0.22)	-5.18 (± 3.32)	0.42 (± 0.04)	-0.68 (± 0.06)	**-1.16 (± 1.46)**	-0.06 (± 0.03)	1.14
52	-9.61 (± 1.05)	-1.10 (± 0.08)	1.1 (+/- 0.52)	-13.10 (± 5.83)	0.05 (± 0.10)	-0.27 (± 0.04)	2.62 (± 0.41)	-0.01 (± 0.00)	-
191	-11.05 (± 0.70)	3.67 (± 0.59)	0.42 (+/- 0.07)	-0.92 (± 0.02)	**-0.06 (± 0.13)**	-0.23 (± 0.01)	5.93 (± 1.37)	**0.04 (± 0.06)**	0.53
209	-9.70 (± 0.74)	12.72 (± 0.03)	0.91 (+/- 0.23)	7.49 (± 1.24)	0.31 (± 0.20)	-0.26 (± 0.23)	2.43 (± 0.50)	-0.04 (± 0.02)	0.96
222	-6.18 (± 0.12)	4.67 (± 0.18)	0.67 (+/- 0.09)	0.56 (± 0.34)	0.29 (± 0.09)	-0.40 (± 0.06)	3.41 (± 2.30)	**0.03 (± 0.07)**	0.61
252	-11.86 (± 1.05)	11.18 (± 10.37)	0.73 (+/- 0.09)	**4.09 (± 12.92)**	-0.40 (± 0.09)	-0.13 (± 0.04)	7.71 (± 2.32)	**-0.02 (± 0.03)**	1.65
265	-11.27	16.21	1.13	5.26	0.28	-0.02	5.34	-0.02	1.34
281	-5.22 (± 0.19)	**2.69 (± 4.24)**	0.51 (+/- 0.03)	**-2.29 (± 3.89)**	-0.23 (± 0.14)	0.01 (± 0.19)	**-0.61 (± 3.53)**	-0.01 (± 0.03)	0.44
305R	-8.99 (± 0.16)	6.36 (± 0.37)	0.73 (+/- 0.12)	1.26 (± 0.38)	-0.02 (± 0.20)	-0.45 (± 0.25)	4.31 (± 1.36)	-0.09 (± 0.01)	1.13
40005	-21.44 (± 1.29)	15.46 (± 7.25)	1.28 (+/- 0.28)	**2.47 (± 6.02)**	1.00 (± 0.61)	-0.90 (± 0.06)	14.15 (± 3.93)	**0.03 (± 0.08)**	1.52
40006	-9.00	2.52	0.35	-1.12	0.13	0.00	4.72	0.01	0.15
40007	-11.89 (± 1.28)	8.99 (± 3.28)	1.06 (+/- 0.09)	**-2.01 (± 4.01)**	-0.17 (± 0.10)	-0.42 (± 0.01)	6.59 (± 0.05)	**0.01 (± 0.02)**	1.33
40008	-12.54	13.14	0.67	7.80	0.65	-0.47	8.70	-0.02	1.25
40009	-18.28	12.96	0.37	8.34	0.70	-0.37	6.73	-0.05	0.95
40010	-5.41	4.27	0.37	0.68	-0.20	-0.49	3.81	-0.01	1.14
40011	-14.47 (± 1.18)	8.58 (± 0.28)	0.73 (+/- 0.16)	**0.69 (± 1.14)**	**0.04 (± 0.09)**	-0.18 (± 0.18)	11.46 (± 1.94)	-0.06 (± 0.02)	1.14
40013	-38.33 (± 0.87)	26.05 (± 0.73)	0.93 (+/- 0.93)	5.68 (± 0.04)	0.49 (± 0.05)	-1.94 (± 0.19)	9.14 (± 0.09)	-0.17 (± 0.00)	4.07
40015	-10.54 (± 0.06)	**10.83 (± 17.00)**	**-0.12 (+/- 0.56)**	**2.52 (± 22.95)**	**-0.07 (± 0.09)**	-0.31 (± 0.13)	8.26 (± 0.07)	0.04 (± 0.02)	1.40
40016	-13.17	3.57	1.02	-6.48	0.21	-0.34	-0.61	-0.04	0.50
40017	-15.35 (± 0.23)	5.40 (± 0.04)	0.67 (+/- 0.07)	-1.35 (± 0.14)	0.25 (± 0.04)	-0.43 (± 0.17)	2.95 (± 0.09)	-0.10 (± 0.03)	0.72
40018	-10.41 (± 1.95)	34.31 (± 27.87)	0.56 (+/- 0.17)	**29.38 (± 30.83)**	-0.11 (± 0.02)	-0.34 (± 0.00)	5.48 (± 1.96)	0.00 (± 0.01)	3.26
40019	-10.38	1.81	0.75	-1.40	1.04	-0.63	3.21	-0.02	-0.21
40020	-9.18 (± 2.22)	4.76 (± 0.92)	0.24 (+/- 0.19)	2.21 (± 1.09)	0.19 (± 0.01)	0.00 (± 0.04)	4.07 (± 1.14)	0.06 (± 0.01)	0.51

Station	Dissolved Oxygen (DO)	Dissolved Inorganic Carbon (DIC)	Hydrogen ion (H^+)	Total Alkalinity (TA)	Ammonium (NH_4^+)	Nitrate +Nitrite (NO_3^-+$NO_2^=$)	Silicate (Si)	Phosphate (PO_4^3)	Estimated Denitrification
40021	-16.87 (± 1.13)	**23.73 (± 26.91)**	1.25 (+/- 0.11)	**15.69 (± 26.37)**	0.92 (± 0.46)	-0.67 (± 0.37)	9.39 (± 0.35)	0.04 (± 0.00)	1.94
40022	-21.57	8.63	1.05	-2.48	1.23	-1.24	14.20	-0.09	1.29
40025	-19.84 (± 1.85)	0.11 (± 0.01)	**0.04 (+/- 0.04)**	-8.60 (± 1.06)	0.80 (± 0.15)	-0.18 (± 0.01)	2.85 (± 0.92)	0.01 (± 0.00)	-0.61
40028	-23.19 (± 0.79)	**3.32 (± 8.83)**	0.93 (+/- 0.10)	-9.12 (± 8.62)	0.32 (± 0.10)	**-0.25 (± 0.25)**	3.86 (± 2.35)	-0.05 (± 0.02)	0.28
40029	-21.73 (± 1.88)	31.83 (± 0.14)	0.75 (+/- 0.11)	24.10 (± 0.34)	0.91 (± 0.19)	-1.15 (± 0.39)	20.29 (± 3.17)	**0.05 (± 0.06)**	4.05
40030	-15.83 (± 0.16)	6.65 (± 1.84)	0.87 (+/- 0.13)	**-1.25 (± 2.70)**	0.93 (± 0.07)	-0.67 (± 0.22)	3.42 (± 0.10)	-0.08 (± 0.02)	0.44
40032	-12.03 (± 0.32)	4.49 (± 0.05)	0.89 (+/- 0.08)	-2.98 (± 0.68)	**-0.13 (± 0.38)**	-0.11 (± 0.05)	2.55 (± 0.55)	**-0.01 (± 0.05)**	0.69
40037	-5.81	11.98	1.12	5.27	0.07	-0.64	4.42	0.01	1.68
40038	-9.31 (± 0.50)	7.51 (± 2.06)	0.57 (+/- 0.07)	1.59 (± 1.39)	0.00 (± 0.10)	-0.21 (± 0.06)	7.76 (± 2.36)	-0.02 (± 0.01)	1.31
BLL009	-13.66 (± 1.90)	12.99 (± 0.57)	0.66 (+/- 0.13)	5.26 (± 0.45)	0.04 (± 0.02)	-0.43 (± 0.22)	6.64 (± 1.74)	0.03 (± 0.01)	2.09
HCB003	-8.72	5.94	0.43	1.79	0.05	-0.12	6.24	0.03	0.59

Table 2. Sampling station coordinates and environmental variables measured at each station in April and early May 2018. BW = bottom water, DO = dissolved oxygen, DIC = dissolved inorganic carbon, TA = total alkalinity, TOC = total organic carbon, TOC:N = total organic carbon to nitrogen ratio.

Station	Latitude (°N)	Longitude (°W)	Depth (m)	BW Temp. (°C)	Salinity (psu)	BW DO (µM)	BW DIC (µM)	BW TA (µM)	BW pH	Total Fines (%)	TOC (%)	TOC:N
4	48.68394	-122.53811	24	9.6	31	259.6	2050.6	2158.2	7.917	82.6	2.1	8.2
13	47.83758	-122.62896	20	10.5	30	252.2	2023.2	2130.2	7.918	11.2	0.2	5.7
19	48.09793	-122.47129	124	9.2	25	212.1	2061.7	2117.2	7.763	65.6	2.0	9.3
21	47.98545	-122.24292	27	9.9	28	261.0	2037.2	2122.7	7.856	61.7	1.2	15.3
29	47.70072	-122.45405	202	9.8	30	249.6	2062.0	2141.8	7.826	73.2	1.8	7.4
34	47.54703	-122.66205	11	9.1	30	286.9	-	-	-	78.2	2.4	9.2
38	47.42835	-122.39361	203	9.3	30	249.4	2056.2	2190.1	7.987	87.6	2.3	7.9
49	47.07997	-122.91353	7	10.0	27	326.7	1925.1	2020.1	7.923	61.7	2.5	9.9
52	47.17059	-122.78061	107	11.0	30	264.7	2021.1	2150.7	7.983	21.8	0.5	8.6
191	47.59842	-122.37578	101	9.0	30	267.5	2022.1	2119.3	7.909	53.5	1.6	11.4
209	48.29534	-122.48857	20	9.5	23	224.6	-	-	-	27.6	0.4	11.4
222	47.67819	-122.81464	127	10.4	30	176.1	2126.6	2161.2	7.659	77.2	1.8	8.4
252	47.26959	-122.85094	55	9.4	30	267.5	2001.7	2086.1	7.876	83.9	2.2	7.7
265	47.25244	-122.66566	108	8.5	31	253.7	2026.4	2105.4	7.868	73.7	2.2	8.1
281	47.29235	-122.44195	140	8.7	30	243.9	2048.4	2130.5	7.860	88.4	1.3	10.8
305R	47.39713	-122.93123	21	11.1	30	123.3	2031.7	2077.9	7.719	76.4	3.6	8.4
40005	48.13872	-123.44985	25	11.0	32	248.8	2079.6	2235.9	8.009	72.0	4.7	17.5
40006	47.63968	-122.49041	81	9.4	31	261.2	2034.5	2122.5	7.874	11.3	0.6	16.5
40007	48.22611	-122.5437	54	9.3	26	233.3	-	-	-	11.9	0.2	10.1
40008	47.22686	-122.64787	125	8.8	30	261.4	1950.3	2023.0	7.859	72.9	2.2	8.1
40009	48.90624	-122.82633	28	9.0	32	-	2031.4	2136.1	7.919	12.1	0.3	6.7
40010	47.59744	-122.97823	134	10.5	27	164.4	2123.4	2175.8	7.720	80.4	2.6	10.7
40011	47.76106	-122.41765	201	9.4	30	242.6	2052.7	2135.1	7.837	67.2	1.6	7.6
40013	48.49623	-122.8214	11	10.5	32	278.8	2031.2	2174.6	8.004	62.9	1.1	8.3
40015	48.08878	-122.44857	108	9.2	25	300.4	2053.8	2181.3	7.991	76.0	2.0	8.7
40016	47.1255	-122.83639	7	10.0	29	325.5	1930.4	2019.5	7.903	83.3	2.7	9.5
40017	48.99472	-122.9678	17	9.0	28	-	2032.4	2155.4	7.972	6.0	0.4	7.1
40018	47.41788	-123.11741	128	12.0	27	91.9	2059.2	2077.8	7.609	86.2	2.3	9.2
40019	47.90608	-122.33067	89	9.3	25	256	2028.0	2117.1	7.885	17.7	0.5	11.1
40020	47.69586	-122.42253	88	9.0	30	255.8	2037.9	2125.0	7.874	6.2	0.3	11.0

Station	Latitude (°N)	Longitude (°W)	Depth (m)	BW Temp. (°C)	Salinity (psu)	BW DO (µM)	BW DIC (µM)	BW TA (µM)	BW pH	Total Fines (%)	TOC (%)	TOC:N
40021	48.27946	-122.61512	13	10.3	28	211.5	1970.8	2025.7	7.777	81.0	1.7	9.5
40022	47.67157	-122.59949	20	9.6	30	265.8	2011.0	2101.0	7.893	92.4	2.9	8.1
40025	48.6245	-122.96328	23	10.1	32	284	2026.0	2104.1	7.821	89.6	1.8	8.9
40028	47.13601	-123.01005	7	10.3	28	395.3	1788.2	1830.5	7.748	85.3	2.7	7.6
40029	48.63714	-122.55224	23	9.6	30	263.1	2041.7	2126.5	7.861	81.8	1.4	7.6
40030	47.54499	-122.65119	11	10.4	29	280.6	2043.1	2147.8	7.910	79.2	3.3	8.7
40032	47.34951	-122.80543	19	9.6	29	244.2	1976.7	2084.5	7.938	14.0	0.4	7.4
40037	48.19993	-122.58646	54	9.4	23	216.3	2055.1	2143.5	7.872	84.9	1.8	9.2
40038	47.69895	-122.47833	187	9.6	29	280.5	2053.9	2146.2	7.864	71.0	1.7	8.2
BLL009	48.68589	-122.59418	19	9.4	29	252.5	2047.3	2148.8	7.912	29.2	0.5	6.0
HCB003	47.59842	-122.37578	101	11.9	29	138.3	2022.1	2119.3	7.909	14.0	1.6	11.4

Table 3. Estimates of sedimentary contribution to bottom water (BW) biogeochemistry for Puget Sound basins in the springtime including removal of BW dissolved inorganic nitrogen (DIN) supply due to denitrification, percentage of particulate phosphorus supplied to sediment that is stored, and percentage of dissolved oxygen (DO) removal caused sediments.

	Nitrogen	**Phosphate**	**DO**
	Percentage of DIN BW supply removed by denitrification (%)	Percentage of supplied particulate phosphate that is stored in sediments (%, ± SE)	Percentage of BW DO removal due to sediments (%)
South Basin	2.7	146 ± 37	80
Central Basin	1.2	94 ± 37	21
Whidbey Basin	2.8	136 ± 46	31
Hood Canal	10.9	111 ± 43	35

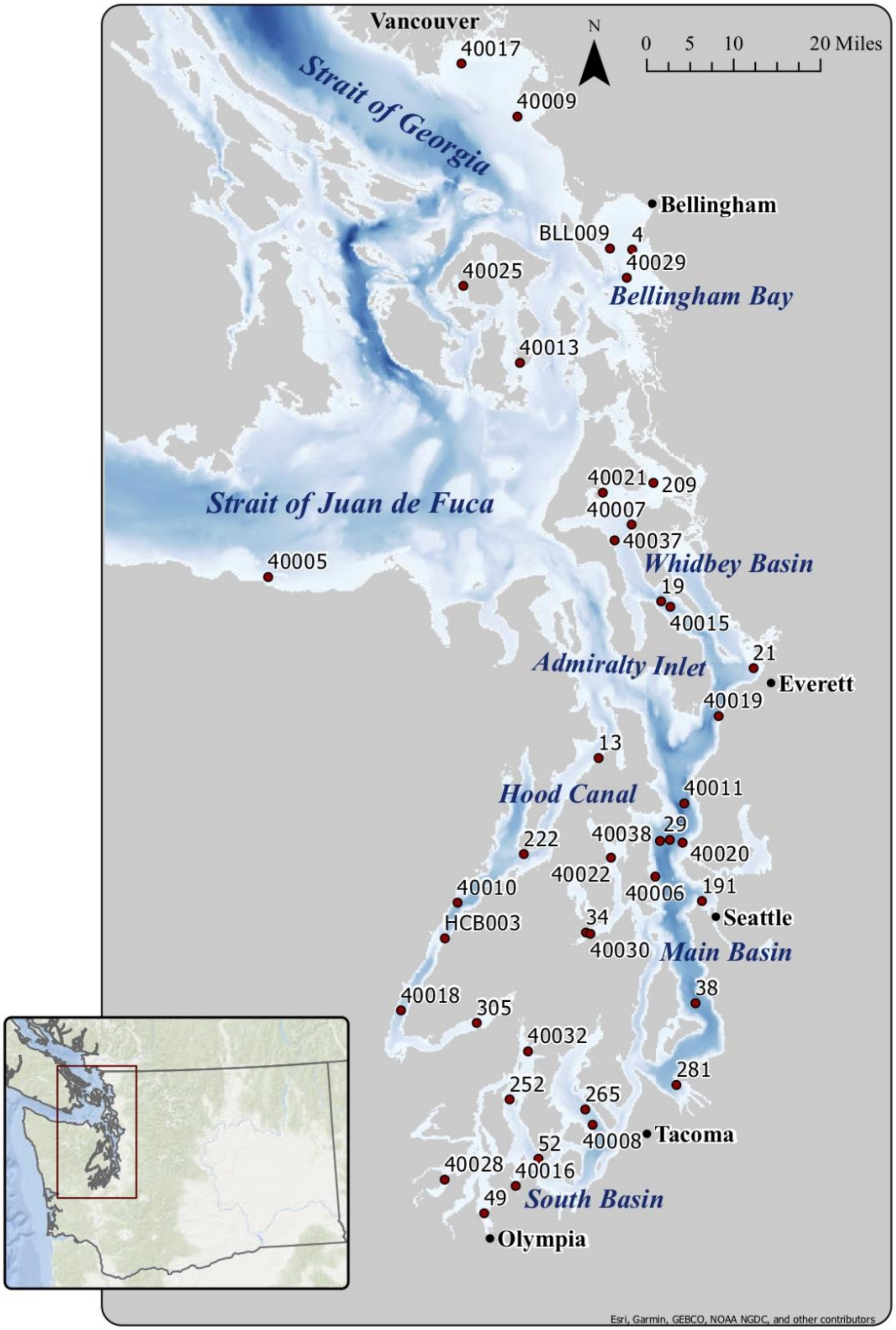

Figure 1. Map of stations sampled in the Salish Sea in April and early May 2018. Bathymetry data from Washington State Department of Fish and Wildlife.

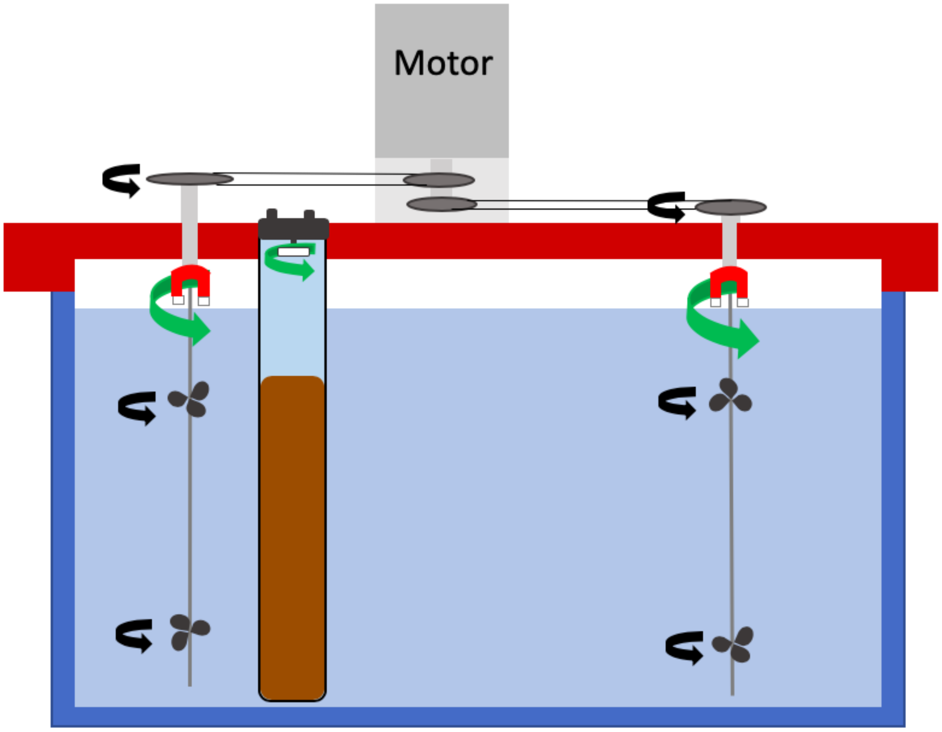

Figure 2. Flux core incubator design using a modified cooler. The motor, located on the top of the lid, rotated horseshoe magnets that created magnetic induction and spun the stir bar located the base of the flux core lids (green arrows). The motor also rotated propellers located in the seawater surrounding the cores to ensure that the temperature throughout the incubator was consistent.

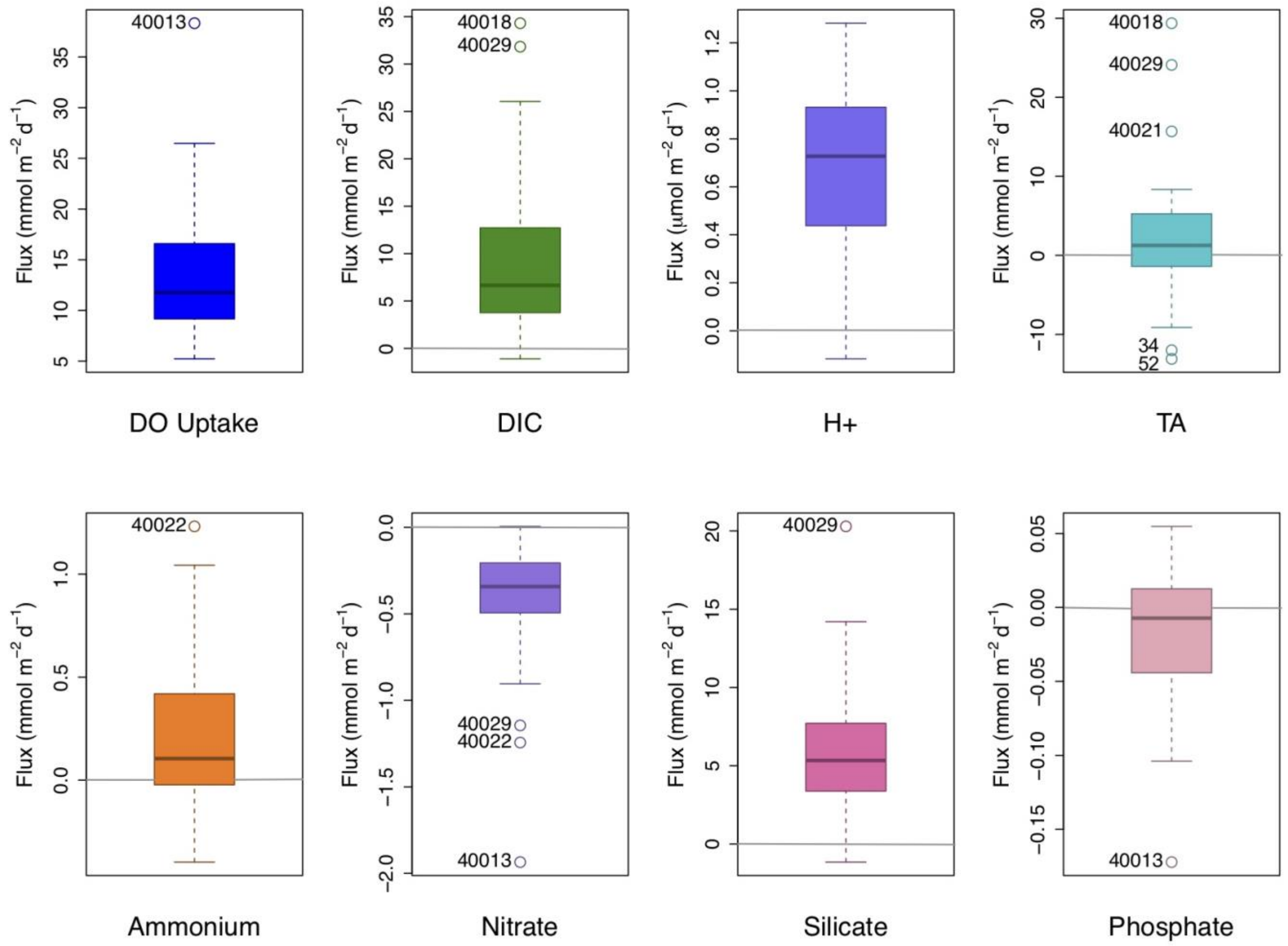

Figure 3. Box plots displaying the distribution and range of measured benthic fluxes. Outlying values are marked with station number. Note the differences in scale for each boxplot. DO = dissolved oxygen, DIC = dissolved inorganic carbon, H^+ = hydrogen ion, TA = total alkalinity.

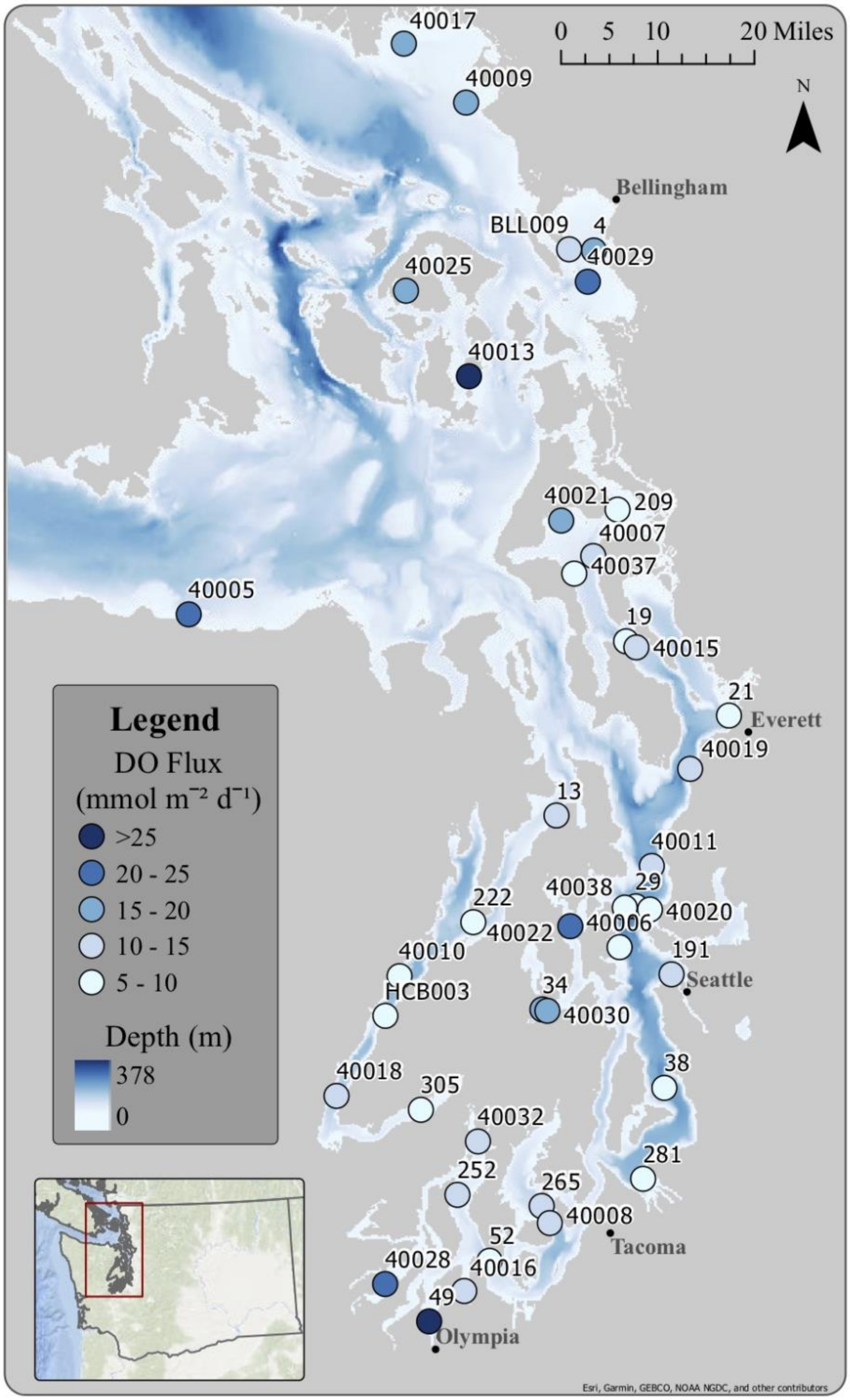

Figure 4. Spatial distribution of dissolved oxygen (DO) benthic uptake in mmol m^{-2} d^{-1}. Bathymetry data from Washington State Department of Fish and Wildlife.

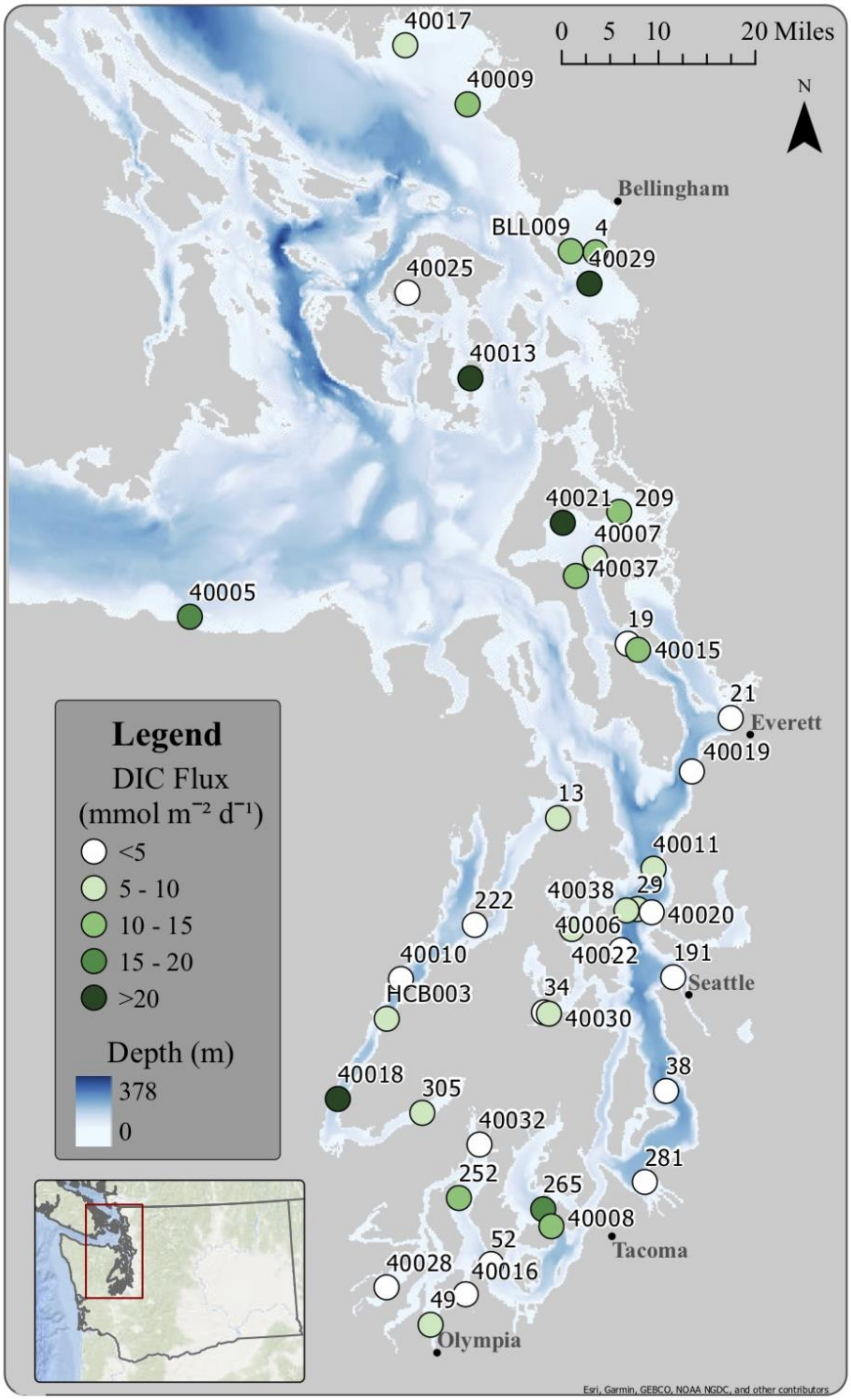

Figure 5. Spatial distribution of dissolved inorganic carbon (DIC) benthic fluxes in mmol m^{-2} d^{-1}. Bathymetry data from Washington State Department of Fish and Wildlife.

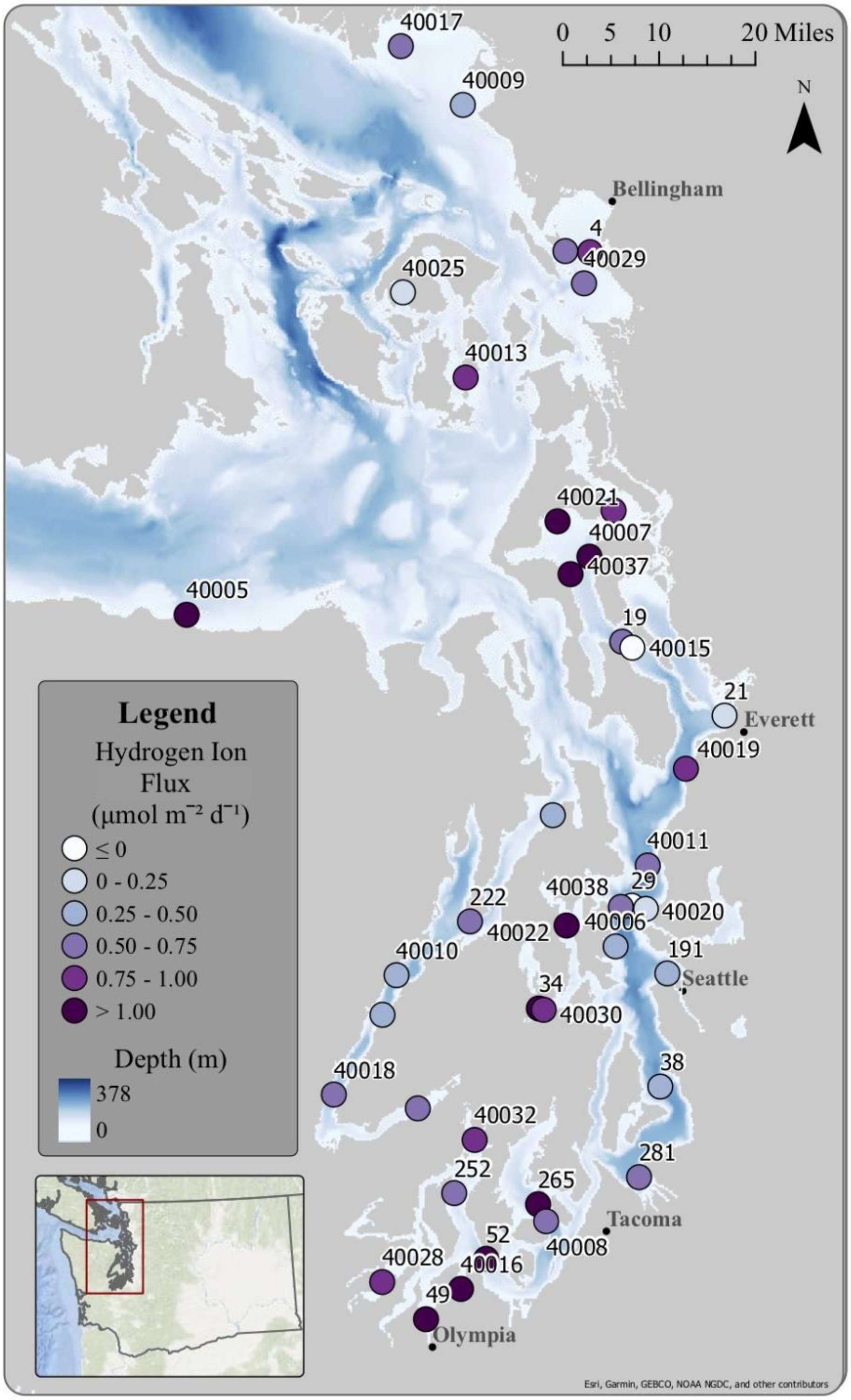

Figure 6. Spatial distribution of hydrogen ion benthic fluxes in µmol m^{-2} d^{-1}. Bathymetry data from Washington State Department of Fish and Wildlife.

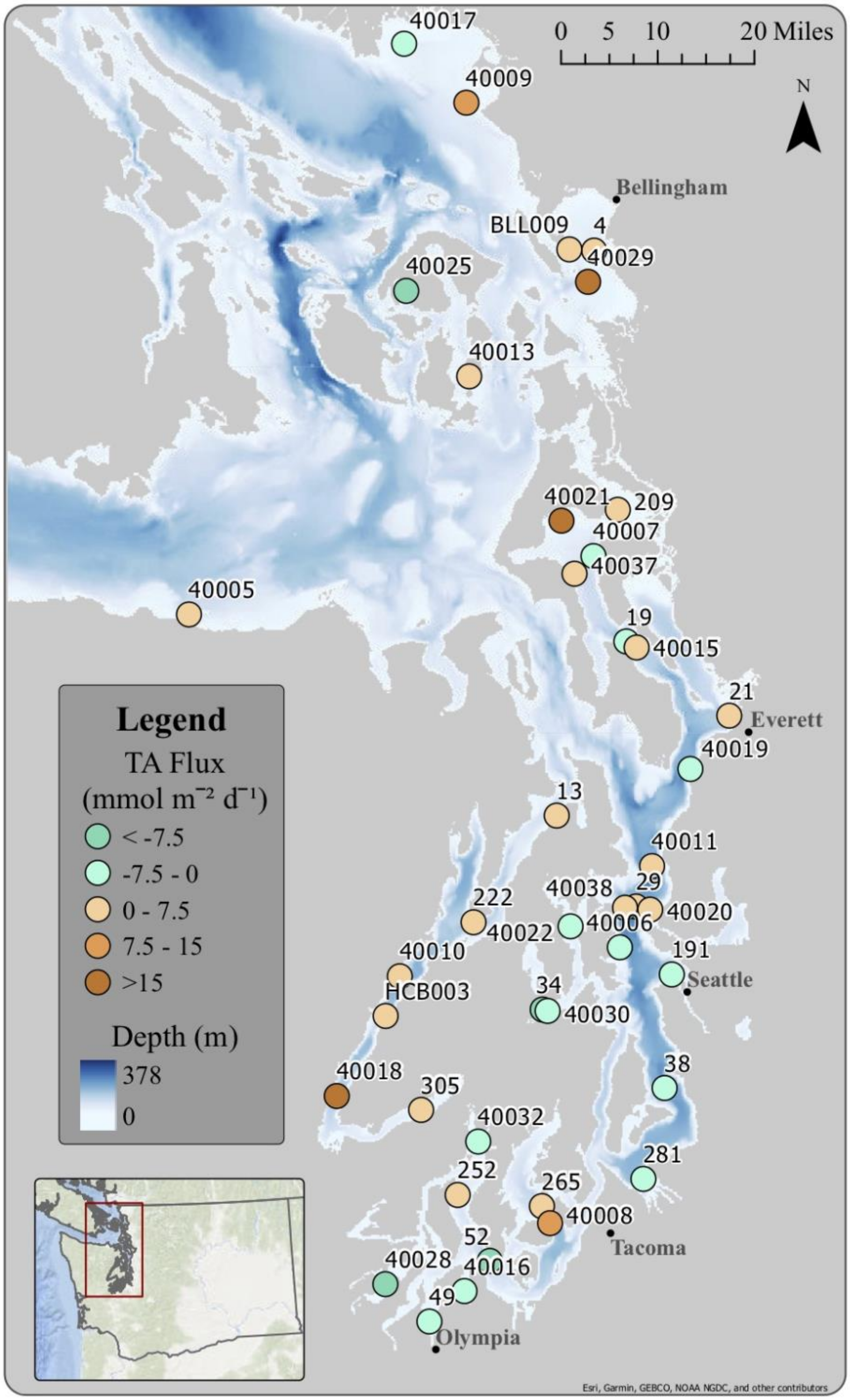

Esri, Garmin, GEBCO, NOAA NGDC, and other contributors

Figure 7. Spatial distribution of total alkalinity (TA) benthic fluxes in mmol m^{-2} d^{-1}. Bathymetry data from Washington State Department of Fish and Wildlife.

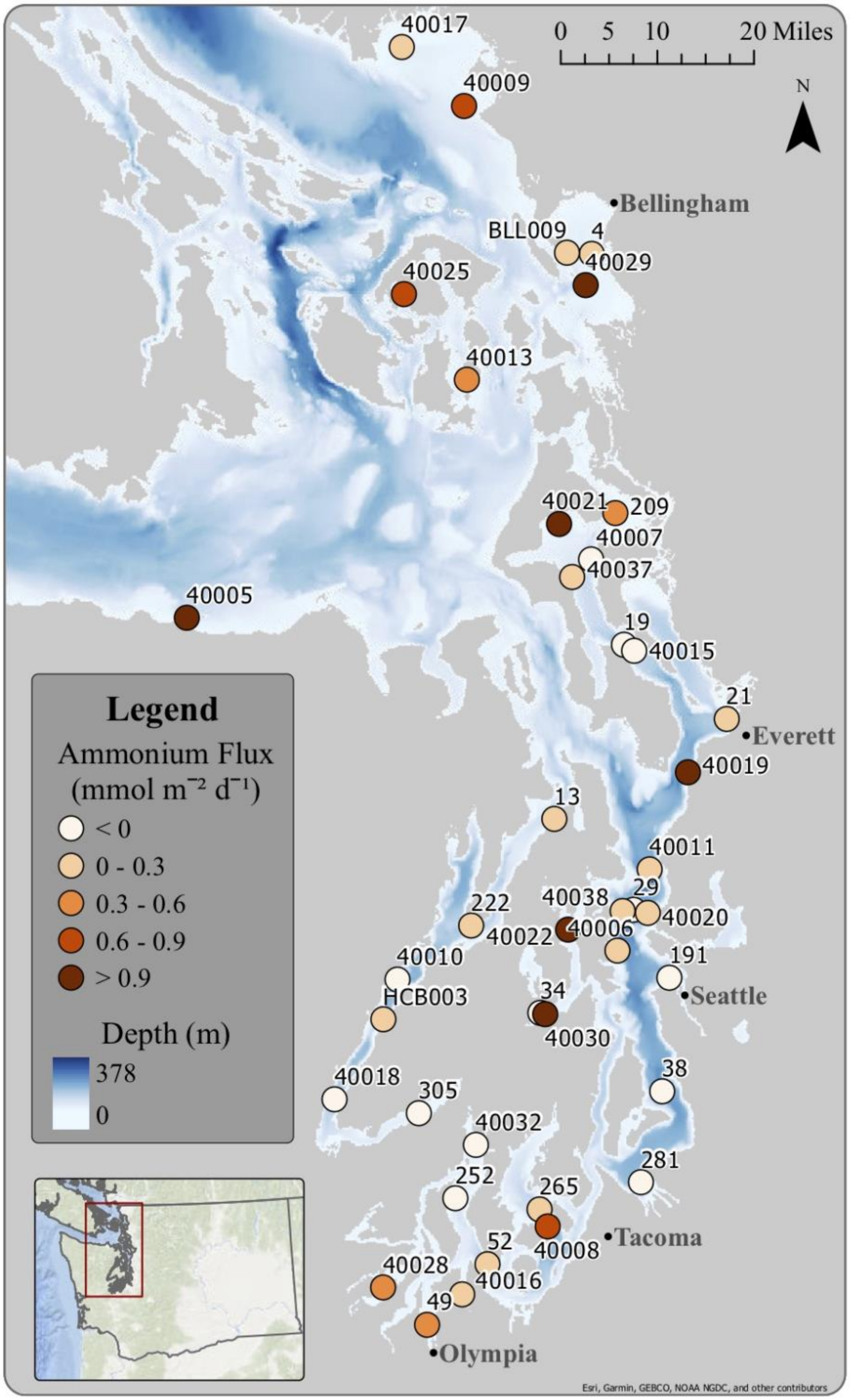

Figure 8. Spatial distribution of ammonium (NH_4^+) benthic fluxes in mmol m^{-2} d^{-1}. Bathymetry data from Washington State Department of Fish and Wildlife.

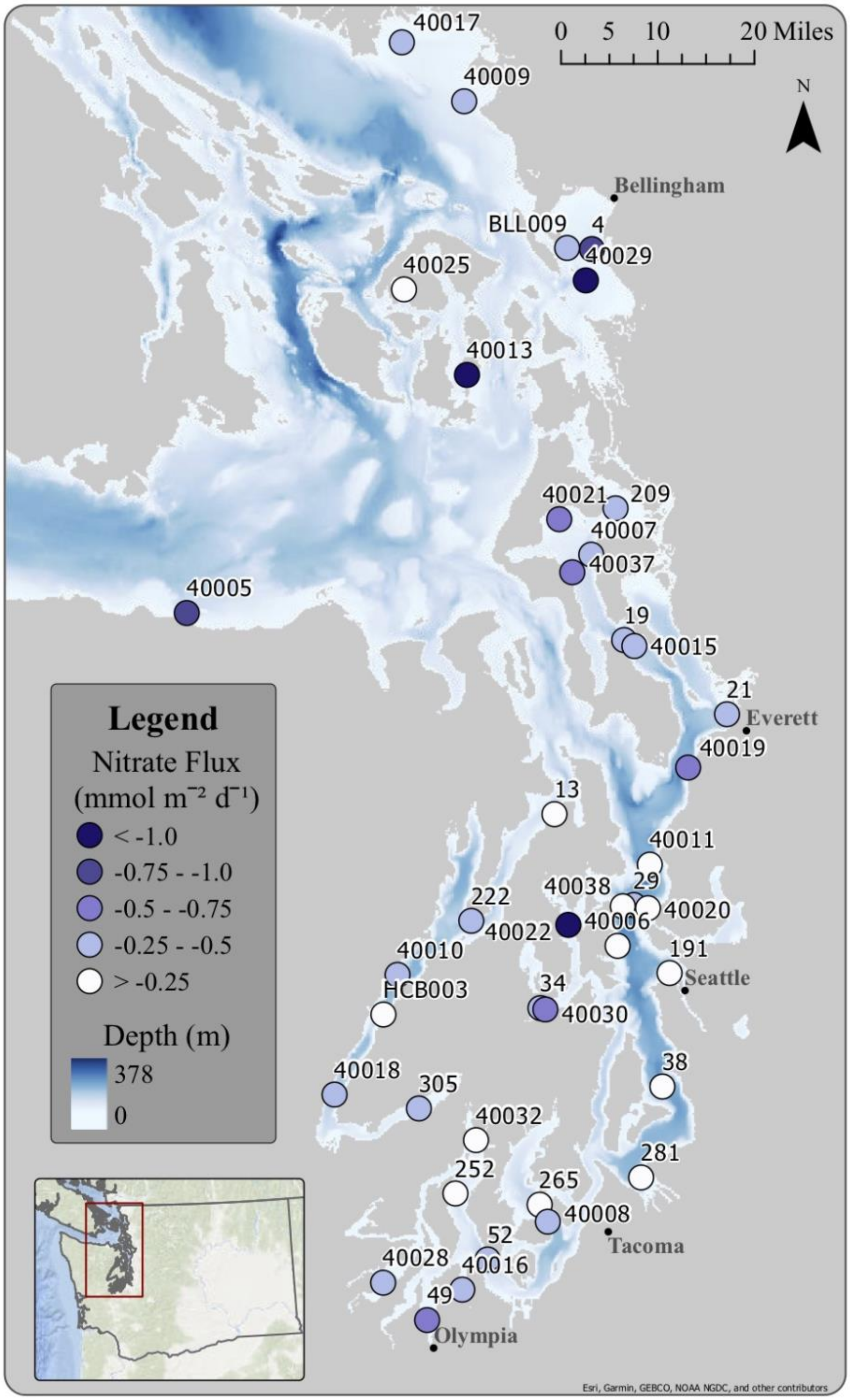

Figure 9. Spatial distribution of nitrate+nitrite ($NO_3^- + NO_2^-$) benthic fluxes in mmol m^{-2} d^{-1}. Bathymetry data from Washington State Department of Fish and Wildlife.

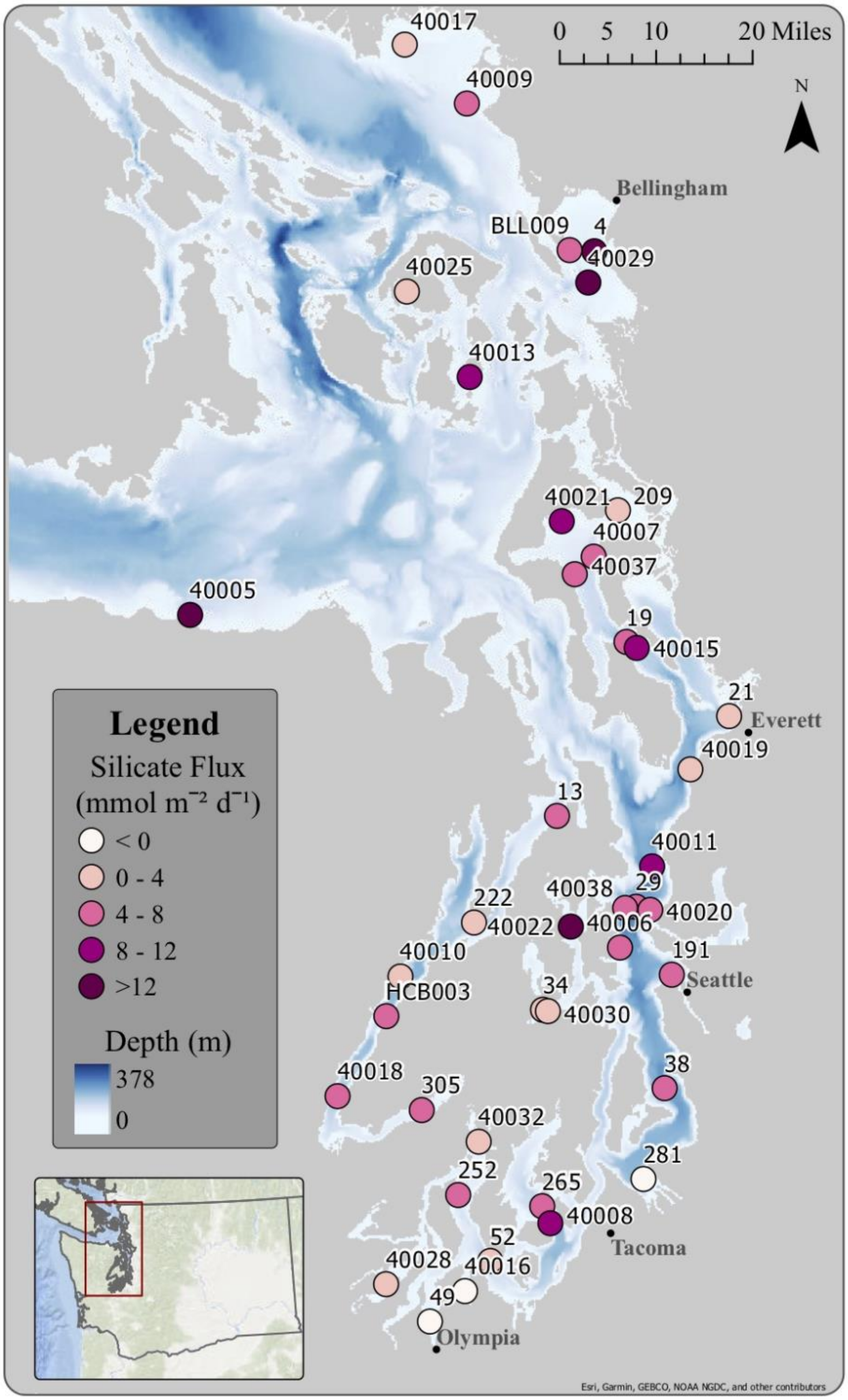

Figure 10. Spatial distribution of silicate benthic fluxes in mmol m^{-2} d^{-1}. Bathymetry data from Washington State Department of Fish and Wildlife.

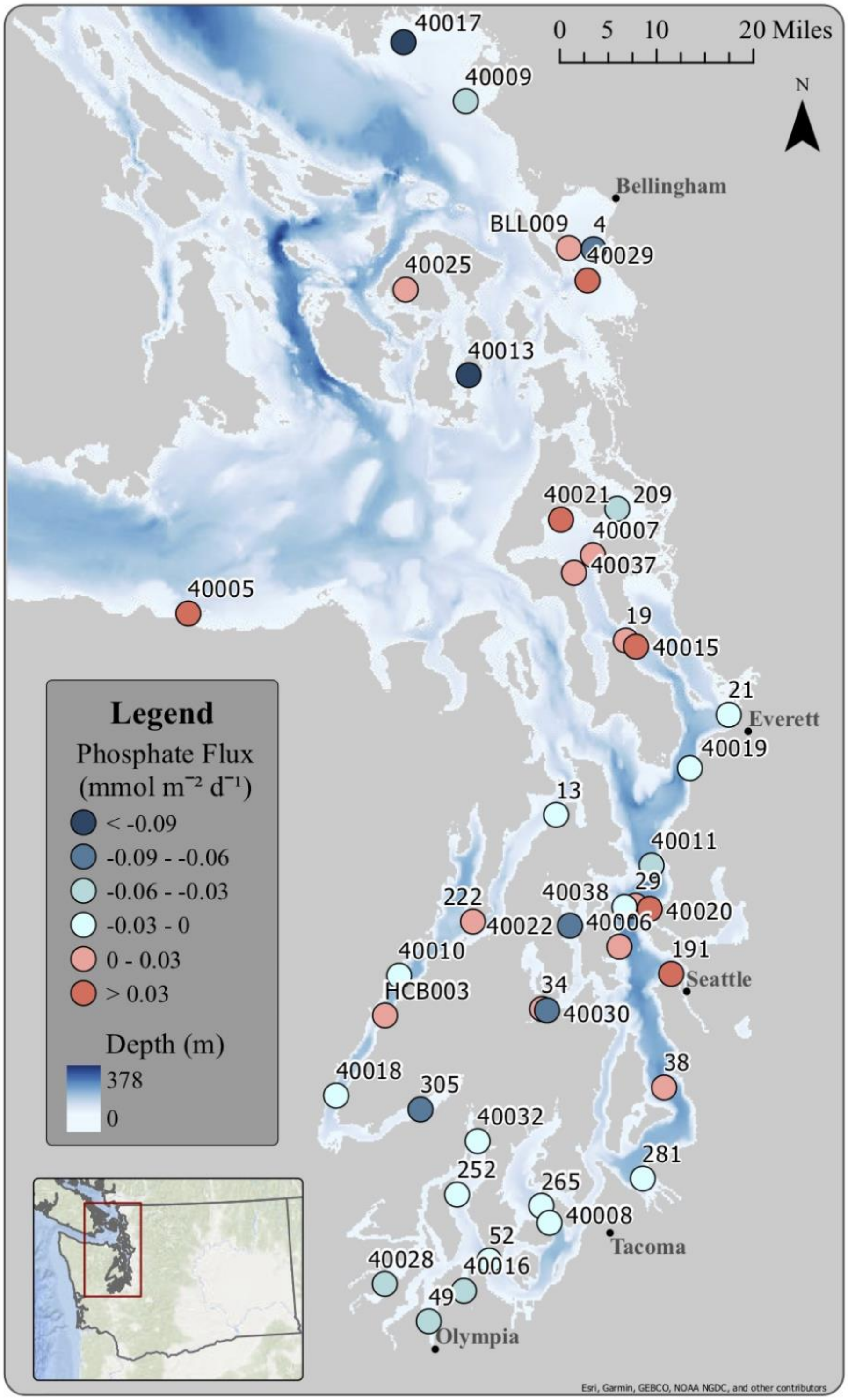

Figure 11. Spatial distribution of phosphate (PO_4^{3-}) benthic fluxes in mmol m^{-2} d^{-1}. Bathymetry data from Washington State Department of Fish and Wildlife.

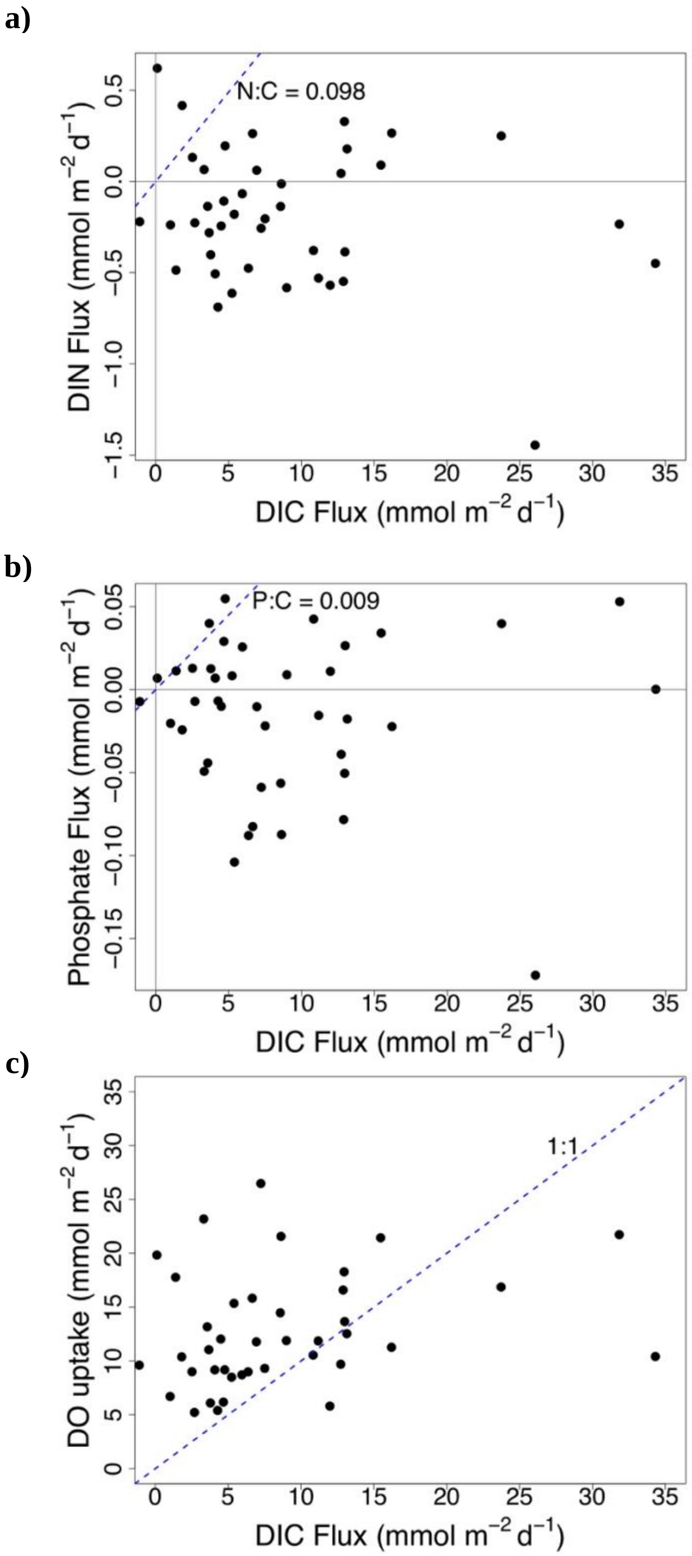

Figure 12. The fluxes of DIN vs. DIC (a), phosphate vs. DIC (b), and DO uptake vs. DIC flux (c) at all of the stations. In DIN vs. DIC fluxes (a), the dashed line displays the annual weighted average of particulate N:C ratios in near bottom water from April 2017 – 2018, which was 0.10. In phosphate vs. DIC fluxes (b), the dashed line is the Redfield ratio of P:C (0.009). In DO uptake vs. DIC flux (c), the dashed line displays the 1:1 relationship.

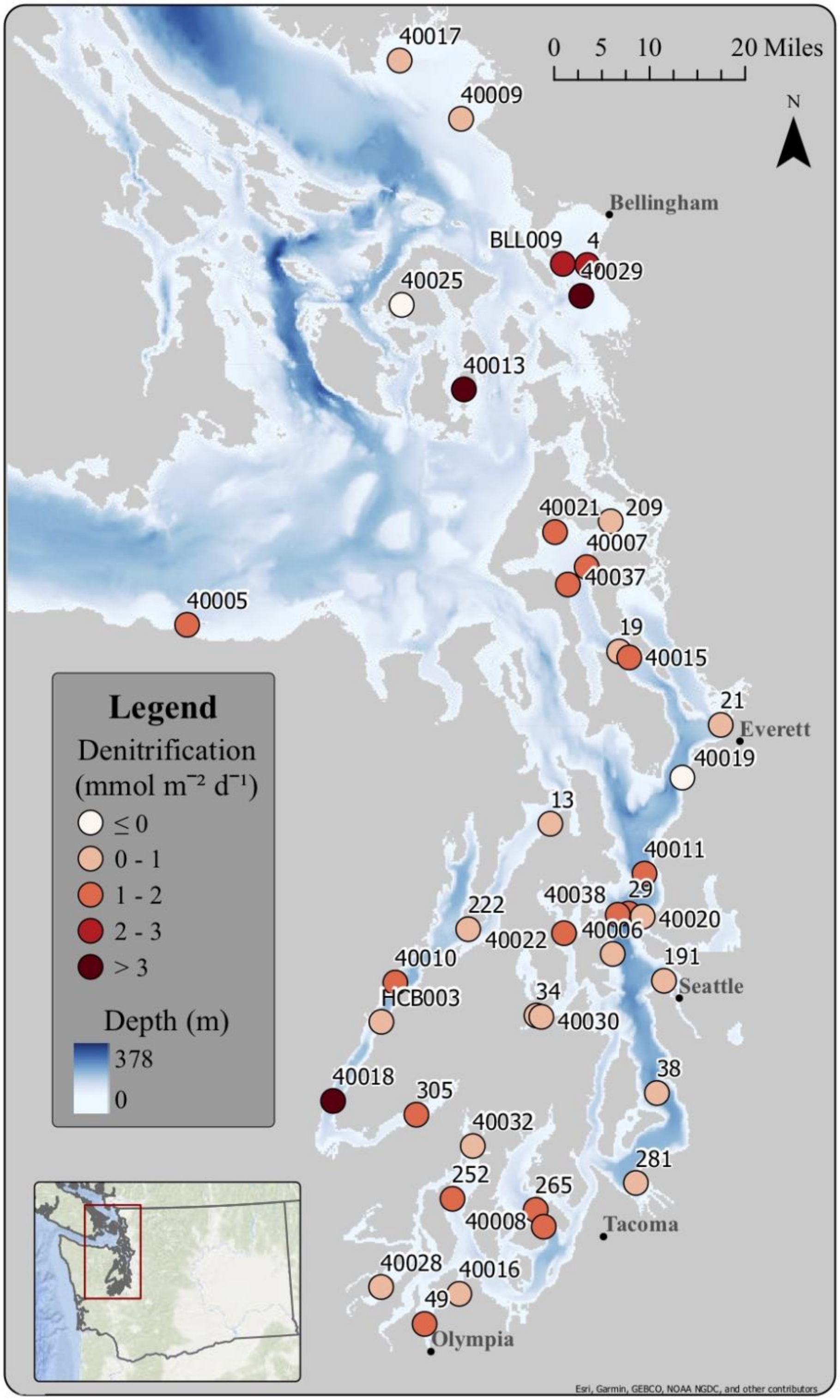

Figure 13. Spatial distribution of denitrification rates in mmol m^{-2} d^{-1}. Bathymetry data from Washington State Department of Fish and Wildlife.

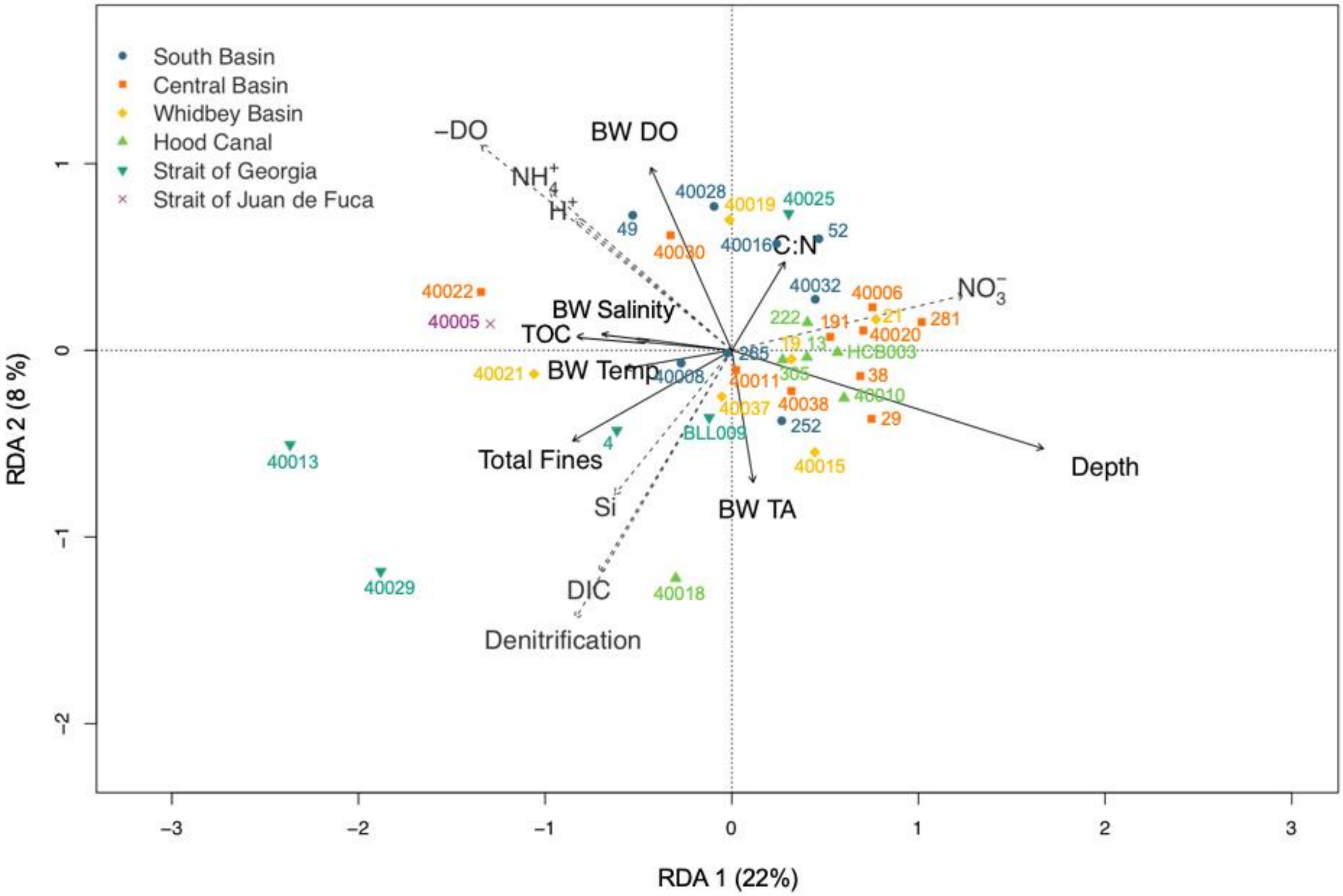

Figure 14. First and second ordination axes of the redundancy analysis (RDA). The first and second axes explain 22% and 8% of the variation, respectively. Black solid lines are environmental variables, black dashed lines are benthic fluxes or the estimated denitrification rate, and points are stations sorted by waterbody.

BW = bottom water, DO = dissolved oxygen, TA = total alkalinity, TOC = total organic carbon in sediment, Temp = temperature, C:N = sediment carbon to nitrogen ratio, -DO = negative dissolved oxygen flux or dissolved oxygen uptake, DIC = dissolved inorganic carbon flux, NH_4^+ = ammonium flux, NO_3^- = nitrate+nitrite flux, Si = silicate flux, H^+ = hydrogen ion flux.

References

Arndt, S., B. B. Jørgensen, D. E. LaRowe, J. J. Middelburg, R. D. Pancost and P. Regnier. 2013. Quantifying the degradation of organic matter in marine sediments: a review and synthesis. Earth-Science Reviews 123: 53-86.

Babbin, A. R., R. G. Keil, A. H. Devol, and B. B. Ward. 2014. Organic matter stoichiometry, flux, and oxygen control nitrogen loss in the ocean. Science 344: 406-408.

Babson, A. L., M. Kawase, and P. MacCready. 2006. Seasonal and interannual variability in the circulation of Puget Sound, Washington: a box model study. Atmosphere-Ocean 44: 29-45.

Batker D., P. Sweeden, R. Costanza, I. de la Torre, R. Boumans, and K. Bagstad. 2008. A new view of the Puget Sound economy: the economic value of nature's services in the Puget Sound basin. Earth Economics, Tacoma, WA. 90 pp.

Belley, R., P. V. Snelgrove, P. Archambault, and S. K. Juniper. 2016. Environmental drivers of benthic flux variation and ecosystem functioning in Salish Sea and Northeast Pacific sediments. PloS one 11: e0151110. https://doi.org/10.1371/journal.pone.0151110.

Berelson, W. M., J. McManus, K. H. Coale, K. S. Johnson, T. Kilgore, D. Burdige and C. Pilskaln. 1996. Biogenic matter diagenesis on the sea floor: A comparison between two continental margin transects. Journal of Marine Research 54: 731-762.

Berelson, W. M., J. McManus, K. H. Coale, K. S. Johnson, D. Burdige, T. Kilgore, D. Colodner, F. Chavez, R. Kudela and J. Boucher. 2003. A time series of benthic flux measurements from Monterey Bay, CA. Continental Shelf Research 23: 457-481.

Berelson, W. M., J. McManus, S. Severmann, and N. Rollins. 2019. Benthic fluxes from hypoxia-influenced Gulf of Mexico sediments: Impact on bottom water acidification. Marine Chemistry 209: 94-106.

Bos, J. 2013. Standard Operating Procedure for Seawater Sampling, Version 2.0. Washington State Department of Ecology Environmental Assessment Program Publication EAP025.

Bos, J., M. Keyzers, L. Hermanson, C. Krembs, and S. Albertson. 2015. Quality Assurance Project Plan: Long-Term Marine Waters Monitoring, Water Column Program. Washington State Department of Ecology, Olympia, WA. Publication 15-03-101. 198 pp. https://fortress.wa.gov/ecy/publications/SummaryPages/1503101.html

Brandes, J.A., and A.H. Devol. 1997. Isotopic fractionation of oxygen and nitrogen in coastal marine sediments. Geochimica et Cosmochimica Acta 61: 1793-1801.

Brenner, H., U. Braeckman, M. Le Guitton and F. J. Meysman. 2016. The impact of sedimentary alkalinity release on the water column CO_2 system in the North Sea. Biogeosciences 13: 841-863.

Burdige, D. J. 2006. Geochemistry of Marine Sediments. Princeton, New Jersey, Princeton University Press. 609 pp.

Cai, W.J. and Y. Wang. 1998. The chemistry, fluxes, and sources of carbon dioxide in the estuarine waters of the Satilla and Altamaha Rivers, Georgia. Limnology and Oceanography 43: 657-668.

Christensen, J. P. and T. T. Packard. 1976. Respiratory electron transport activities in phytoplankton and bacteria: Comparison of methods 1. Limnology and Oceanography 24: 576-583.

Christensen, P. B., S. Rysgaard, N. P. Sloth, T. Dalsgaard and S. Schwærter. 2000. Sediment mineralization, nutrient fluxes, denitrification and dissimilatory nitrate reduction to ammonium in an estuarine fjord with sea cage trout farms. Aquatic Microbial Ecology 21: 73-84.

Clayton, T. D. and R. H. Byrne. 1993. Spectrophotometric seawater pH measurements: total hydrogen ion concentration scale calibration of m-cresol purple and at-sea results. Deep Sea Research Part I: Oceanographic Research Papers 40: 2115-2129.

Cornwell, J. C., W. M. Kemp and T. M. Kana. 1999. Denitrification in coastal ecosystems: methods, environmental controls, and ecosystem level controls, a review. Aquatic Ecology 33: 41-54.

Devol, A. H., 2015. Denitrification, anammox, and N2 production in marine sediments. Annual Review of Marine Science 7: 403-423.

Dollar, S. J., S. V. Smith, S. M. Vink, S. Obrebski, and J. T. Hollibaugh. 1991. Annual cycle of benthic nutrient fluxes in Tomales Bay, California, and contribution of the benthos to total ecosystem metabolism. Marine Ecology Progress Series 79: 115-125.

Dutch, M., S. Weakland, V. Partridge, D. Burgess, and A. Eagleston. 2018. Quality Assurance Project Plan: Revisions to the Puget Sound Sediment Monitoring Program. Washington State Department of Ecology, Olympia, WA. Publication 18-03-105. 128 pp. https://fortress.wa.gov/ecy/publications/SummaryPages/01803105.html.

Duxbury, A. C. 1987. A Fjord-like Estuary. NOAA Estuary of the Month Publications, Seminar Series No. 8: 1-11.

Engström, P., C.R. Penton and A.H. Devol. 2009. Anaerobic ammonium oxidation in deep-sea sediments off the Washington margin. Limnology and Oceanography, 54: 1643-1652.

Faul, K. L., A. Paytan, and M. L. Delaney. 2005. Phosphorus distribution in sinking oceanic particulate matter. Marine Chemistry 97: 307-333.

Feeley, R. A., S. R. Alin, J. Newton, C. L. Sabine, M. Warner, A. Devol, C. Krembs, and C. Maloy. 2010. The combined effects of ocean acidification, mixing, and respiration on pH and carbonate saturation in an urbanized estuary. Estuarine, Coastal and Shelf Science 88: 442-449.

Giblin, A. E., C. S. Hopkinson, and J. Tucker. 1997. Benthic metabolism and nutrient cycling in Boston Harbor, Massachusetts. Estuaries 20: 346-364.

Giblin, A. E., C. R. Tobias, B. Song, N. Weston, G. T. Banta, and V. H. Rivera-Monroy. 2013. The importance of dissimilatory nitrate reduction to ammonium (DNRA) in the nitrogen cycle of coastal ecosystems. Oceanography 26: 124-131.

Gordon, L. I., J. C. Jennings Jr, A. A. Ross, and J. M. Krest. 1993. A suggested protocol for continuous flow automated analysis of seawater nutrients (phosphate, nitrate, nitrite and silicic acid) in the WOCE Hydrographic Program and the Joint Global Ocean Fluxes Study. WOCE Operations Manual Part 3: 91-1.

Green, M. A., and R. C. Aller. 2001. Early diagenesis of calcium carbonate in Long Island Sound sediments: Benthic fluxes of Ca2+ and minor elements during seasonal periods of net dissolution. Journal of Marine Research 59: 769-794.

Grebmeier, J. M., C. P. McRoy, and H. M. Feder. 1988. Pelagic-benthic coupling on the shelf of the northern Bering and Chukchi seas. 1. Food supply source and benthic biomass. Marine Ecology Progress Series 48: 57-67.

Hamilton, E. L., 1976. Variations of density and porosity with depth in deep-sea sediments. Journal of Sedimentary Research 46: 280-300.

Hammond, D. E., C. Fuller, D. Harmon, B. Hartman, M. Korosec, L.G. Miller, R. Rea, S. Warren, W. Berelson, and S. W. Hager. 1985. Benthic fluxes in San Francisco bay. Temporal dynamics of an estuary. In: San Francisco Bay. Springer, Dordrecht. pp. 69-90.

Hammond, D. E., J. McManus, W. M. Berelson, T. E. Kilgore and R. H. Pope. 1996. Early diagenesis of organic material in equatorial Pacific sediments: stoichiometry and kinetics. Deep Sea Research Part II: Topical Studies in Oceanography 43: 1365-1412.

Horak, R. E., H. Whitney, D. H. Shull, C. W. Mordy, and A. H. Devol. 2013. The role of sediments on the Bering Sea shelf N cycle: insights from measurements of benthic denitrification and benthic DIN fluxes. Deep Sea Research Part II: Topical Studies in Oceanography 94: 95-105.

Joye, S. B., S. V. Smith, J. T. Hollibaugh and H. W. Paerl. 1996. Estimating denitrification rates in estuarine sediments: a comparison of stoichiometric and acetylene based methods. Biogeochemistry 33: 197-215.

Keyzers, M. 2017. Quality Assurance Project Plan: Addendum 4 to Quality Assurance Monitoring Plan, Long-Term Marine Waters Monitoring, Water Column Program. Washington State Department of Ecology, Olympia, WA. Publication No. 17-03-103. 46 pp. https://fortress.wa.gov/ecy/publications/SummaryPages/1703103.html

Krumins, V., M. Gehlen, S. Arndt, P. V. Cappellen and P. Regnier. 2013. Dissolved inorganic carbon and alkalinity fluxes from coastal marine sediments: model estimates for different shelf environments and sensitivity to global change. Biogeosciences 10: 371-398.

Legendre, P., and L. Legendre. 1998. Numerical Ecology: Second English edition. Developments in Environmental Modelling. 852 pp.

Lowe, A. T., J. Bos and J. Ruesink. 2019. Ecosystem metabolism drives pH variability and modulates long-term ocean acidification in the Northeast Pacific coastal ocean. Scientific Reports 9: 963. https://doi.org/10.1038/s41598-018-37764-4.

Mackas, D. L. and P. J. Harrison. 1997. Nitrogenous nutrient sources and sinks in the Juan de Fuca Strait/Strait of Georgia/Puget Sound estuarine system: assessing the potential for eutrophication. Estuarine, Coastal and Shelf Science 44: 1-21.

Marino, R. and R. W. Howarth. 2016. Why Is Planktonic Nitrogen Fixation So Rare in Coastal Marine Ecosystems? Insights from a Cross-Systems Approach. In Aquatic Microbial Ecology and Biogeochemistry: A Dual Perspective. Switzerland, Springer International Publishing. 127-139 pp.

Middelburg, J. J., K. Soetaert, P. M. Herman and C. H. Heip. 1996. Denitrification in marine sediments: A model study. Global Biogeochemical Cycles 6: 569-570.

Middelburg, J. J. and L. A. Levin. 2009. Coastal hypoxia and sediment biogeochemistry. Biogeosciences 6: 1273-1293.

Millero, F.J., 2010. Carbonate constants for estuarine waters. Marine and Freshwater Research 61: 139-142

Mohamedali, T., M. Roberts, B. Sackmann, and A. Kolosseus. 2011. Puget Sound Dissolved Oxygen Model Nutrient Load Summary for 1999-2008. WA State Department of Ecology Pub. No. 11-03-057. 172 pp.

Nakata, K., and J. A. Newton. 2000. Seasonal patterns and controlling factors of primary production in Puget Sound’s Central Basin and Possession Sound. In: T. Droscher, (ed.) Puget Sound Water Quality Action Team, 2002. Proceedings of the 2001 Puget Sound Research Conference. Puget Sound Water Quality Action Team. Olympia, Washington. 9pp.

Newton, J., C. Bassin, A. Devol, M. Kawase, W. Ruef, M. Warner, D. Hannafious and R. Rose. 2007. Hypoxia in Hood Canal: An overview of status and contributing factors. Proceedings of the 2007 Georgia Basin Puget Sound Research Conference. 10 pp.

Nixon, S. W. 1981. Remineralization and nutrient cycling in coastal marine ecosystems. In: Estuaries and Nutrients, Humana Press, pp. 111-138.

Norkko, J., J. Gammal, J. E. Hewitt, A. B. Josefson, J. Carstensen and A. Norkko. 2015. Seafloor ecosystem function relationships: In situ patterns of change across gradients of increasing hypoxic stress. Ecosystems 18: 1424-1439.

Pamatmat, M. M. 1971. Oxygen consumption by the seabed. VI. Seasonal cycle of chemical oxidation and respiration in Puget Sound. Int. Rev. Hydrobiology 56: 769-793.

Pierrot, D., E. Lewis, and D. W. R. Wallace. 2006. MS Excel Program Developed for CO2 System Calculations. ORNL/CDIAC-105a. Carbon Dioxide Information Analysis Center, Oak Ridge National Laboratory, U.S. Department of Energy, Oak Ridge, Tennessee. doi: 10.3334/CDIAC/otg.CO2SYS_XLS_CDIAC105a

PSEMP Marine Waters Workgroup. 2018. Puget Sound marine waters: 2017 overview. S. K. Moore, R. Wold, K. Stark, J. Bos, P. Williams, N. Hamel, A. Edwards, C. Krembs, and J. Newton, editors. URL: www.psp.wa.gov/PSmarinewatersoverview.php. 56 pp.

Rabalais, N. N., R. E. Turner, R. J. Diaz, and D. Justić. 2009. Global change and eutrophication of coastal waters. ICES Journal of Marine Science 66: 1528-1537.

Rabalais, N. N., R. J. Diaz, L. A. Levin, R. E. Turner, D. Gilbert and J. Zhang. 2010. Dynamics and distribution of natural and human-caused hypoxia. Biogeosciences 7: 585 - 619.

Roberts, L. and M. Elliott. 2017. Good or bad vibrations? Impacts of anthropogenic vibration on the marine epibenthos. Science of the Total Environment 595: 255-268.

Sheibley, R.W. and A. J. Paulson. 2014. Quantifying benthic nitrogen fluxes in Puget Sound, Washington: a review of available data. Publication No. 2014-5033. US Geological Survey. 43 pp.

Smith, V. H., S. B. Joye and R. W. Howarth. 2006. Eutrophication of freshwater and marine ecosystems. Limnology and Oceanography 51: 351-355.

Sohm, J. A., E. A. Webb and D. G. Capone. 2011. Emerging patterns of marine nitrogen fixation. Nature Reviews Microbiology 97: 499 - 508.

Stevens, D. L. and A. R. Olsen. 2004. Spatially balanced sampling of natural resources. Journal of the American Statistical Association 99: 262-278.

Strickland, R. 1983. The Fertile Fjord, Plankton in Puget Sound. Washington Sea Grant. Seattle, WA. University of Washington Press, WA. 145 pp.

Suess, E. 1980. Particulate organic carbon flux in the oceans—surface productivity and oxygen utilization. Nature 288: 260 - 263.

Sundby, B., C. Gobeil, N. Silverberg, and A. Mucci. 1992. The phosphorus cycle in coastal marine sediments. Limnology and Oceanography 37: 1129-1145.

Sutton, J. N., S. C. Johannessen, and R. W. Macdonald. 2013. A nitrogen budget for the Strait of Georgia, British Columbia, with emphasis on particulate nitrogen and dissolved inorganic nitrogen. Biogeosciences 10: 7179-7194.

Turner, R. E., N. Qureshi, N. N. Rabalais, Q. Dortch, D. Justic, R. F. Shaw and J. Cope. 1998. Fluctuating silicate: nitrate ratios and coastal plankton food webs. Proceedings of the National Academy of Sciences 95: 13048-13051.

Wallace, R. B., H. Baumann, J. S. Grear, R. C. Aller and C. J. Gobler. 2014. Coastal ocean acidification: The other eutrophication problem. Estuarine, Coastal and Shelf Science 148: 1-13.